CHAPTER 7

Systems vaccinology reveals superior protection after pulmonary compared to subcutaneous administration of an outer membrane vesicle pertussis vaccine associated with local and systemic immune signatures in mice

René H.M. Raeven[1,5,#], Jolanda Brummelman[2,4,#], Jeroen L.A. Pennings[3], Larissa van der Maas[1], Kina Helm[2], Wichard Tilstra[1], Arno van der Ark[1], Arjen Sloots[1], Peter van der Ley[1], Willem van Eden[4], Wim Jiskoot[5], Elly van Riet[1], Cécile A.C.M. van Els[2], Gideon F.A. Kersten[1,5], Wanda G.H. Han[2,*], Bernard Metz[1,*]

[1]Intravacc, Institute for Translational Vaccinology, Bilthoven, The Netherlands,
[2]Centre for Infectious Disease Control, National Institute for Public Health and the Environment, Bilthoven, The Netherlands,
[3]Centre for Health Protection, National Institute for Public Health and the Environment, Bilthoven, The Netherlands,
[4]Department of Infectious Diseases and Immunology, Utrecht University, The Netherlands,
[5]Division of Drug Delivery Technology, Leiden Academic Centre for Drug Research, Leiden, The Netherlands
[#] Authors contributed equally
[*] Authors contributed equally

Submitted for publication

Abstract

Local immune responses in the lungs contribute to protection against *B. pertussis* infection and might improve the vaccine-elicited immunity. Therefore, the effect of the vaccine administration route on the degree of protection and the local and systemic immune response was investigated. Immunization of mice via the pulmonary route with a novel outer membrane vesicle pertussis vaccine (omvPV) led to faster clearance of *B. pertussis* upon intranasal challenge compared to immunization via the subcutaneous route. The local and systemic immune responses underlying this difference in protection were analyzed using a systems biology approach. Exclusively pulmonary immunization led to the presence of *B. pertussis*-specific IgA antibodies, IgA-producing plasma cells and Th17-cells in the lungs. Moreover, this route elicited increased levels of systemic specific IgG antibodies, IgG-producing plasma cells, memory B-cells, and Th17-cells. In addition, only pulmonary immunization elicited a rapid induction of pro-inflammatory cytokines and chemoattractants, e.g. IL-6 and CXCL10, observed on transcriptomic and proteomic levels, in the lungs. Distinct cytokine profiles were measured in sera, which were overall higher after subcutaneous immunization, e.g. G-CSF and IL-5. Transcriptome analysis of lungs and draining lymph nodes revealed differences in innate and adaptive responses between both administration routes e.g. the expression of *Igha* and *Rorc*, supporting the superior IgA, IgG, and Th17 responses detected in pulmonary-immunized mice. These results show that by administering the vaccine via the pulmonary as opposed to the subcutaneous route, an omvPV can elicit superior local and systemic immunity against *B. pertussis*, resembling immunity after primary infection. The study indicates that pulmonary immunization may be key to improve pertussis vaccination strategies.

Introduction

Currently, pertussis remains an endemic disease, even in highly vaccinated populations. Approaches to increase protection include the improvement of pertussis vaccines and vaccination strategies [1, 2]. The whole-cell and acellular pertussis vaccines induce a systemic immune response characterized by the formation of IgG antibodies and a T-helper (Th) response that is Th1/Th17 or Th2 dominated, respectively [3-6]. In contrast, a *B. pertussis* infection evokes a Th1/Th17 response both systemically and locally in the lungs [5, 7, 8]. Outer-membrane vesicle pertussis vaccines (omvPV) might be an improved alternative for the currently available vaccines. Subcutaneous immunization of omvPV elicited a systemic immune response comparable to that induced by *B. pertussis* infection, including high serum IgG levels against a broad antigen range [9] and a mixed Th1, Th17, and Th2 response [10]. Unfortunately, subcutaneous omvPV immunization does not induce local immune responses in the lungs that are thought to contribute to a better protection against *B. pertussis* [10].

Direct vaccine administration in the respiratory tract can lead to better protection compared to parenteral administration due to the induction of local immune responses as was shown for other respiratory pathogens, such as *M. tuberculosis* and influenza [11-13]. The feasibility of mucosal administration of different pertussis vaccines was proven as intranasal immunization provides protection against *B. pertussis* challenge [14-17]. Nonetheless, direct comparison of the local and systemic immune responses induced by parental and mucosal immunization of pertussis vaccines is not yet performed.

In the present study, we investigated in detail whether the route of immunization affects protection and the quality of the immune response in mice. A systems biology approach was used to compare immune responses following pulmonary and subcutaneous immunization with omvPV (**Figure 1A**). Such an approach was previously applied in vaccine research to predict vaccine responsiveness [18-21] and to unravel of molecular signatures of mucosal adjuvants [22] and respiratory pathogen infections [7, 23]. In our study, the novel omvPV-P93 with abolished Prn autocleavage was used, since it enables more specific readouts and provides better protection in a murine challenge model compared to the WT omvPV, even at a lower dose [24]. Besides *B. pertussis* clearance from the respiratory tract after intranasal challenge, gene expression profiles in draining lymph nodes and lungs, and cytokine profiles and antibody responses in serum and lungs of immunized mice were determined. Finally, specific B-cell and T-cell responses were investigated both locally and systemically. Our results demonstrate hallmarks of superior protective immunity to *B. pertussis* conferred by pulmonary vaccination with omvPV.

Materials and Methods

Vaccine and antigens

The outer membrane vesicle pertussis vaccine (omvPV) was prepared using a genetically modified *B. pertussis* B1917 strain lacking the autocleavage site in pertactin (Prn), as described previously [24]. 1 µg total protein omvPV was diluted in 50 µl and 300 µl PBS (Gibco) for pulmonary and subcutaneous immunization respectively. Pertussis antigens Ptx and FHA were obtained from Kaketsuken (Japan), Prn and Fim2/3 were kindly provided by Betsy Kuipers (National Institute for Public Health and the Environment, Bilthoven, the Netherlands).

B. pertussis challenge culture

The *B. pertussis* challenge culture was prepared as described in the literature [7], except that bacteria were grown in THIJS medium [25].

Ethics statement

An independent ethical committee for animal experimentations of the Institute for Translational Vaccinology (Intravacc) approved the animal experiments with identifiers 201400125 and 201400182. Animal handling in this study was carried out in accordance to the guidelines provided by the Dutch Act on Animal Experimentation.

Immunization and challenge of mice

Female BALB/c mice (Harlan, The Netherlands), 8-week-old, were immunized with 1 µg total protein omvPV either pulmonary (P.M.; 50 µl) or subcutaneously (S.C.; 300 µl) on day 0 and 28. Non-immunized (N.I.) mice were used as a control. Pulmonary administration was performed as described by Bivas-Benita *et al.* [26] using a MicroSprayer aerosolizer (IA-1C; Penn-Century, Philadelphia, PA, USA) supplied with a high-pressure syringe (FMJ-250; Penn-Century). Mice were intranasally challenged under anesthesia (isoflurane/oxygen), with 2×10^5 colony forming units (cfu) of *B. pertussis* B1917 in 20 µL of THIJS medium on day 56.

For gene expression in the lungs and draining lymph nodes (dLN), cytokine responses, and antibody responses, mice (n = 4 per group) were sacrificed 4 hours and 2, 7, 14 and 28 days after primary immunization. In addition, to investigate gene expression in the dLN, cytokine responses, and antibody responses after booster vaccination, mice (n = 4 per group) were sacrificed on day 35 and 56. Finally, mice (n = 4 per group) were sacrificed 4 hours after challenge and on day 58, 63, 70, and 84 to measure bacterial load in the respiratory tract, cytokine responses and antibody responses. For evaluation of B-cell responses, mice (n = 6 per group) were sacrificed on day 35 and 63 (plasma cells) and on day 56 and 84 (memory B-cells). For investigation of T-cell responses, mice (n = 6 per group) were sacrificed on day 28, 56, and 84. An additional control group (n = 6) of completely naive mice were included for B- and T-cell investigation on each time point. Mice were bled under anesthesia (isoflurane/

oxygen) by orbital bleeding and sacrificed by cervical dislocation for further sample collection. An overview of the study design of treatment and sample collection is schematically depicted in Figure 1A.

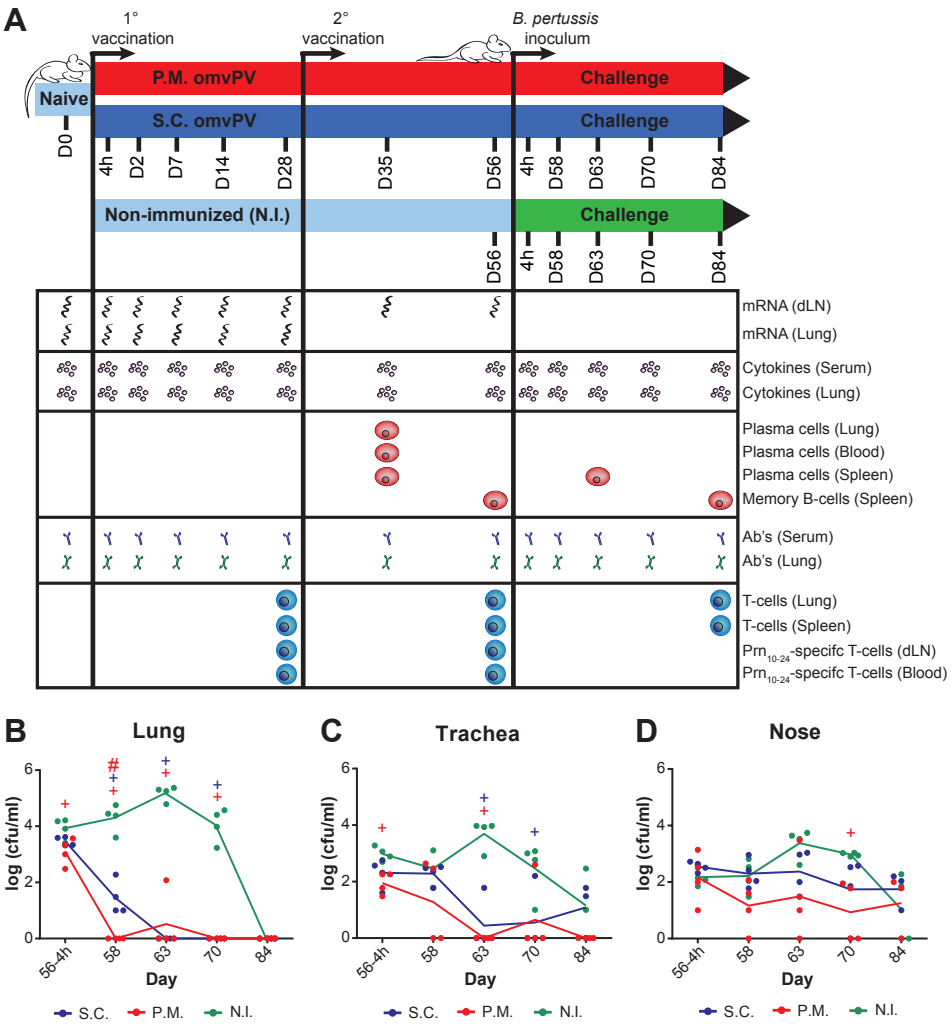

Figure 1 - Study design and *B. pertussis* colonization measured in the respiratory tract. **(A)** BALB/c mice were immunized with 1 µg omvPV pulmonary (P.M.; red) or subcutaneously (S.C.; blue) twice on day 0 and day 28. Subsequently, for both routes the vaccination-induced responses were characterized over a period of 56 days at 7 different time points. Additionally, a *B. pertussis* challenge ($2x10^5$ CFU) was performed on day 56 in both vaccinated groups and non-immunized (N.I.) mice (green). Vaccination responses and *in vivo* recall responses were characterized at the transcriptomic, proteomic and cellular level on given time points, as depicted. **(B-D)** The number of colony-forming units (cfu) were determined after *B. pertussis* challenge **(B)** in lungs, **(C)** trachea and **(D)** nose lavages of S.C. and P.M. immunized and N.I. mice. # $p \leq 0.05$ versus S.C. mice; + $p \leq 0.05$ versus N.I. mice.

Sample collection

From the lungs, the left lobe was placed in 1 ml RNAlater (Qiagen), incubated overnight at 4°C, and stored at -80°C for subsequent microarray analysis. The right lobe was collected in 900 µl THIJS medium and was homogenized using a Bio-Gen PRO200 Homogenizer (Pro Scientific Inc., Oxford, CT, USA) for the lung colonization assay after the challenge and after filtration (Millex GV Filter unit 0.22 µm, Millipore), lysates of all time points were used for pulmonary cytokine and antibody analysis. Complete lungs of mice used for T- and B-cell assays were collected in 5 ml RPMI-1640 medium (Gibco) supplemented with 10% FCS (Hyclone), 100 units penicillin, 100 units streptomycin, and 2.92 mg/ml L-glutamine (Invitrogen), hereafter named RPMI complete medium and kept on ice until use. The draining lymph nodes (dLN), bronchial LN for P.M. immunization and inguinal LN for S.C. immunization, were isolated and placed in 5 ml RPMI complete medium and kept on ice until use, for subsequent microarray analysis and T-cell analysis by tetramer staining. Whole blood for tetramer staining and analysis of B-cell responses was collected in heparin tubes (MiniCollect 1 ml LH Lithium Heparin, Greiner Bio-One, Austria). Serum for cytokine and antibody responses was obtained by collecting whole blood in a serum collection tube (MiniCollect 0.8 ml Z Serum Sep GOLD, Greiner Bio-One, Austria). After coagulation (10 min. at room temperature), sera were taken after centrifugation (10 min., 3000 g) and stored at -80°C. Spleens were placed in 5 ml RPMI complete medium and kept on ice for subsequent B- and T-cell assays. Trachea were collected in 900 µl THIJS medium and were homogenized using the Bio-Gen PRO200 Homogenizer for the trachea colonization assay. Nose lavage was obtained by flushing the nose with 1 ml THIJS medium after the trachea was removed for nose colonization assay. After filtration (Millex GV Filter unit 0.22 µm, Millipore), nose lavages were used to determine nasal antibody responses.

Colonization assays

The tissue lysates from lungs and trachea, and lavages of the nose were serially diluted (undiluted, 1:10, 1:100, and 1:1000) in THIJS medium. The diluted samples were plated on Bordet-Gengou agar plates and incubated for 5 days at 35°C. The number of cfu per ml was determined by using a colony counter (ProtoCOL, Synbiosis, Cambridge, United Kingdom).

B-cell ELISpot

Wells of filter plates (Multiscreen-HA 96 wells plates, Millipore) were coated (overnight, 4°C) with 5 µg/ml Prn (Sanofi) or 10 µg/ml wildtype B1917 OMV. As a positive control, wells were coated with a mixture of 7 µg/ml purified goat-anti-mouse kappa and 7 µg/ml purified goat-anti-mouse lambda (Southern Biotech). As a negative control, wells were left uncoated (PBS). After washing 3 times with PBS, the plates were blocked (1h, room temperature (RT)) with RPMI 1640 + 2% Protifar (Nutricia) and washed again.

Spleens and lungs were homogenized using a 70-µm cell strainer (BD Falcon, BD Biosciences) and cells were collected in RPMI complete medium. From whole blood, erythrocytes were lysed by using RBC lysis buffer (Pharm Lyse, BD Pharmingen). For detection of memory B-cells, $5x10^5$ splenocytes per well of a 24 well-plate were stimulated with CpG ODN 1826 (10 µg/mL, Invivogen), PWM (10 µg/mL), Staphylococcus aureus protein A of Cowan Strain (1:5000) and β-mercaptoethanol (1:25000) (all Sigma) in RPMI complete medium for 5 days at 37ºC to induce antibody secretion. Cells from blood ($0.75x10^5$ cells/well), lungs ($0.75x10^5$ cells/well), spleen ($5x10^5$ cells/well) or stimulated splenocytes ($5x10^5$ cells/well) were added to the coated plates and incubated overnight at 37°C. Plates were washed 7 times with PBS and 3 times with PBS-T (0.05% Tween-20). Then, the plates were incubated (1h, 37°C) with alkaline phosphatase-conjugated goat-anti-mouse IgA or IgG (Southern Biotech; 1:1000). Plates were washed 7 times with PBS, 3 times with PBS-T, and 5 times with tap water. Subsequently, filtered (0.45 µm) BCIP-NBT liquid substrate (Sigma) was added. Spot development was stopped by removing the substrate and extensively rinsing with distilled water. Plates were dried and stored at room temperature in the dark. Spots were counted with an AID iSpot reader (Autoimmun Diagnostika GmbH). The number of *B. pertussis* OMV-specific IgG- and IgA-secreting cells were indicated as antibody secreting cells (ASC) per 5 x 10^5 cells.

Antibody measurements

OMV-, Prn-, FHA-, Ptx-, and Fim2/3-specific antibodies were measured using an in-house developed mouse multiplex immunoassay, as described previously [27]. Serum samples were diluted 1:5000 for IgG (subclass) and 1:100 for IgM and IgA measurements. Lung lysate samples were diluted 1:100 and nose lavage samples were not diluted for measuring IgA levels. Reporter antibodies were R-PE-conjugated goat-anti-mouse IgA, IgG, IgG1, IgG2a, IgG2b, IgG3 or IgM (Southern Biotech). Data were acquired with a Bio-Plex 200, analyzed using Bio-Plex Manager software (version 5.0, Bio-Rad Laboratories), and presented as fluorescence intensities (FI).

Detection of Prn_{10-24} -specific $CD4^+$ T-cells

dLN were homogenized using a 70-µm cell strainer and cells were collected in RPMI complete medium. Blood was treated with erythrocyte-lysis buffer (10 g/L NH_4CL, 1.25 g/L $NaHCO_3$, 0.125 mM EDTA in dH_20; pH 7.4) for 10 minutes on ice, and then resuspended in RPMI complete medium. Cells were stained with APC-conjugated I-A^d tetramers specific for the Prn_{10-24} T-cell epitope [28] (NIH Tetramer Facility, Atlanta, Georgia, USA) in RPMI complete medium for 1 hour at 37°C. Next, cells were stained with Pacific blue-conjugated anti-CD4 (Biolegend), FITC-conjugated anti-CD44 (BD Biosciences), and LIVE/DEAD® Fixable Aqua Dead Cell Stain Kit for 30 minutes at 4°C in FACS buffer (PBS (pH 7.2) supplemented with 0.5% BSA (Sigma Aldrich) and 0.5 mM EDTA (ICN Biomedicals). Data were acquired on a FACS Canto II (BD Biosciences) and analyzed using FlowJo software (Tree Star).

Intracellular cytokine staining (ICS)

Lungs and spleens were homogenized using a 70-µm cell strainer and cells, collected in RPMI complete medium, were treated with erythrocyte lysis buffer. The cells were cultured in 24-well plates ($6x10^6$ cells/well) for 3 days at 37°C in the presence of IMDM complete medium (IMDM medium (Gibco) supplemented with 8% FCS, 100 units penicillin, 100 units streptomycin, 2.92 mg/ml L-glutamine, and 20 µM β-mercaptoethanol (Sigma)). For restimulation of cells, 1 µg/ml Prn or 1.5 µg/ml wildtype B1917 OMVs was added. On day 3, supernatant was collected for cytokine analysis, and the cells were transferred to U-bottom 96-well plates ($5x10^5$ cells/well) and restimulated overnight using the same antigen conditions.

ICS was performed on restimulated splenocytes and lung cells by using the BD Cytofix/Cytoperm Fixation/Permeabilization Solution Kit (BD Biosciences), according to the manufacturer's protocol. Briefly, cells were incubated with 10 µg/ml Golgiplug (BD Biosciences), 1 µg/ml αCD28 (BD Pharmingen), and 1 µg/ml αCD49d (BD Pharmingen) during the last 5 hours of restimulation. Cells were then stained in FACS buffer with Pacific blue-conjugated anti-CD4 (Biolegend), FITC-conjugated anti-CD44 (BD Biosciences), PE-Cy7-conjugated anti-CD103 (Biolegend; only the lung cells), and with LIVE/DEAD Fixable Aqua Dead Cell Stain Kit (Invitrogen). Thereafter, cells were fixed, permeabilized, and stained with PE-conjugated anti-IFNγ (BD Biosciences), APC-conjugated anti-IL-5 (Biolegend), and PerCP-Cy5.5-conjugated anti-IL-17A (eBioscience). Data were acquired on a FACS Canto II and analyzed by using FlowJo software.

Multiplex cytokine analysis (MIA)

Concentrations (pg/ml) of 32 cytokines (Eotaxin, G-CSF, GM-CSF, IFNγ, IL-10, IL-12 (p40), IL-12 (p70), IL-13, IL-15, IL-17A, IL- 1α, IL-1β, IL-2, IL-3, IL-4, IL-5, IL-6, IL-7, IL-9, IP-10, KC, LIF, LIX, M-CSF, MCP-1, MIG, MIP-1α, MIP-1β, MIP-2, RANTES, TNFα, and VEGF) present in serum and lung lysates were determined by using a MIA (Milliplex MAP Mouse Cytokine/ Chemokine - Premixed 32 Plex; Merck KGaA). The concentration of various Th subset cytokines (IL-4, IL-5, IL-10, IL-13, IL-17A, TNFα, and IFNγ) was determined in splenic culture supernatant using a Milliplex mouse cytokine 7-plex luminex kit (Millipore), according to the manufacturer's protocol. Measurements and data analysis were performed with a Bio-Plex 200 and using Bio-PlexManager software (version 5.0, Bio-Rad Laboratories). Results of the Th subset cytokines were corrected for the background (IMDM complete medium control) per mouse per stimulation per cytokine and calculated in pg/ml.

RNA isolation and microarray analysis

Isolation of RNA from lung tissue with additional determination of RNA concentrations and integrity was performed as described previously [7]. For isolation of RNA from cells in the dLN, the dLN were homogenized using a 70-µm cell strainer (BD Falcon, BD Biosciences) and cells were collected in RPMI complete medium and then washed with PBS. By using the MagNA Pure LC RNA Isolation High Performance kit (Roche) according to the manufactures protocol,

the cells were lysed, in 1 ml lysis buffer, and RNA was isolated with the MagNA Pure System (Roche). For lung tissue, samples of naive mice and P.M. vaccinated mice were analyzed as individual samples (n=3), whereas the RNA concentrates of S.C. vaccinated mice were pooled (n=3) for the following time points: Naive, 4 hours, 2 days, 7 days, 14 days, and 28 days post primary vaccination. RNA concentrates from the lymph node suspensions, bronchial for P.M. vaccination and inguinal for S.C. vaccination, of individual mice (n=3) were analyzed for eight time points (naive, 4 hours, 2 days, 7 days, 14 days, 28 days, 35 days and 56 days post primary vaccination). From the naive mice, both bronchial and inguinal lymph nodes were analyzed. Amplification, labeling and hybridization of RNA samples for either lung tissue or lymph nodes for microarray (HT MG-430 PM Array Plates, Affymetrix, Santa Clara, Calif, USA) was carried out at the Microarray Department of the University of Amsterdam, The Netherlands.

Transcriptomic data analysis

Quality control and normalization of raw Affymetrix CEL files were performed using the ArrayAnalysis website (www.arrayanalysis.org) [29], using the Robust Multichip Average (RMA) method [30] and the MBNI custom CDF version 19 [31]. Normalized data consisted of Log2 transformed signal values for 17856 genes. Subsequent analysis of normalized data was performed in R (www.r-project.org) and Microsoft Excel. To identify differentially expressed genes between experimental groups (naive and various time points post vaccination) an ANOVA was applied. The induction or repression of individual genes was expressed as fold ratio by comparing mean gene expression levels of experimental groups to the naive mice. For pulmonary transcriptome analysis, average normalized gene expression levels contain individual data of three mice per group (P.M. and naive mice) and pooled data of 3 mice for the S.C. group. For dLN transcriptome analysis, average normalized gene expression levels contain individual data of three mice per group. The criteria for differential expression for the pulmonary transcriptome analysis were *p*-value <0.01 (ANOVA) and an absolute fold ratio >2.0 (experimental groups compared to naive mice). For dLN transcriptome analysis, the criteria were set at *p*-value < 0.001 and fold ratio > 1.5. GeneMaths XT (Applied Maths, St-Martens-Latem, Belgium) was used to visualize differences in gene expression in heatmaps. Genes were arranged according to similar expression patterns in time at which genes exceeded the fold ratio cut-off. To facilitate visual interpretation of heatmaps, upregulation (red) and downregulation (green) of gene expression levels are only visualized above the fold ratio cutoffs and presenting fold ratios below the cutoffs as an unchanged value (black). Additional data visualization was done by principal component analysis based on expression profiles of all differentially expressed genes in R. Functional enrichment was determined with an over-representation analysis (ORA) based on Gene Ontology Biological Processes (GO-BP) and Kyoto Encyclopedia of Genes and Genomes (KEGG) by using DAVID [32]. Involvement of type I and II interferon-signaling pathway was performed by using the Interferome database (http://www.interferome.org/interferome/home.jspx) [33].

Gene network analysis

To construct a gene-function network, genes associated with five modules, namely acute phase, cytokine response, humoral response, pathogen recognition receptor (PRR) signaling, and T-cell responses, were determined using the ORA results and additional text mining. Interactions between genes were determined using the STRING database (http://string.embl.de/) with high confidence (0.700) and using co-occurrence, co-expression, experiments, databases, and text mining as types of evidence. Gene-function associations and gene-gene interactions were combined into one network file. The network visualization was performed using Cytoscape (version 2.8.3).

Immunoproteomic profiling

One-dimensional (1D) and two-dimensional (2D) electrophoresis in combination with Western blotting (1DEWB, 2DEWB) and LC-MS analysis were performed for the identification of antigen specificity of the antibody responses as described in the literature [9]. Acrylamide gels were loaded with 10-15 µg protein of a *B. pertussis* (B1917) lysate for 1D and with 25 µg protein of the lysate for 2D electrophoresis and blotted. Blots were treated with diluted sera (1:100), diluted lung lysates (1:10-1:50) and diluted nose lavages (1:10) prior to immunostaining with two different IR-800-labeled goat-anti-mouse secondary antibodies (anti-IgG or -IgA). Blots were scanned using an Odyssey infrared imager (Westburg) and analyzed with Delta2D software (Version 4.5) (Decodon, Germany).

Statistics

To determine significance of differences in the outcome of B-cell ELIspot, T-cell ICS, and T-cell tetramer analysis between groups, a Mann-Whitney t-test was used. Data of the cytokine, antibody, and colonization assays were log-transformed after which a t-test was performed. *p*-values ≤0.05 were considered to indicate significance of differences.

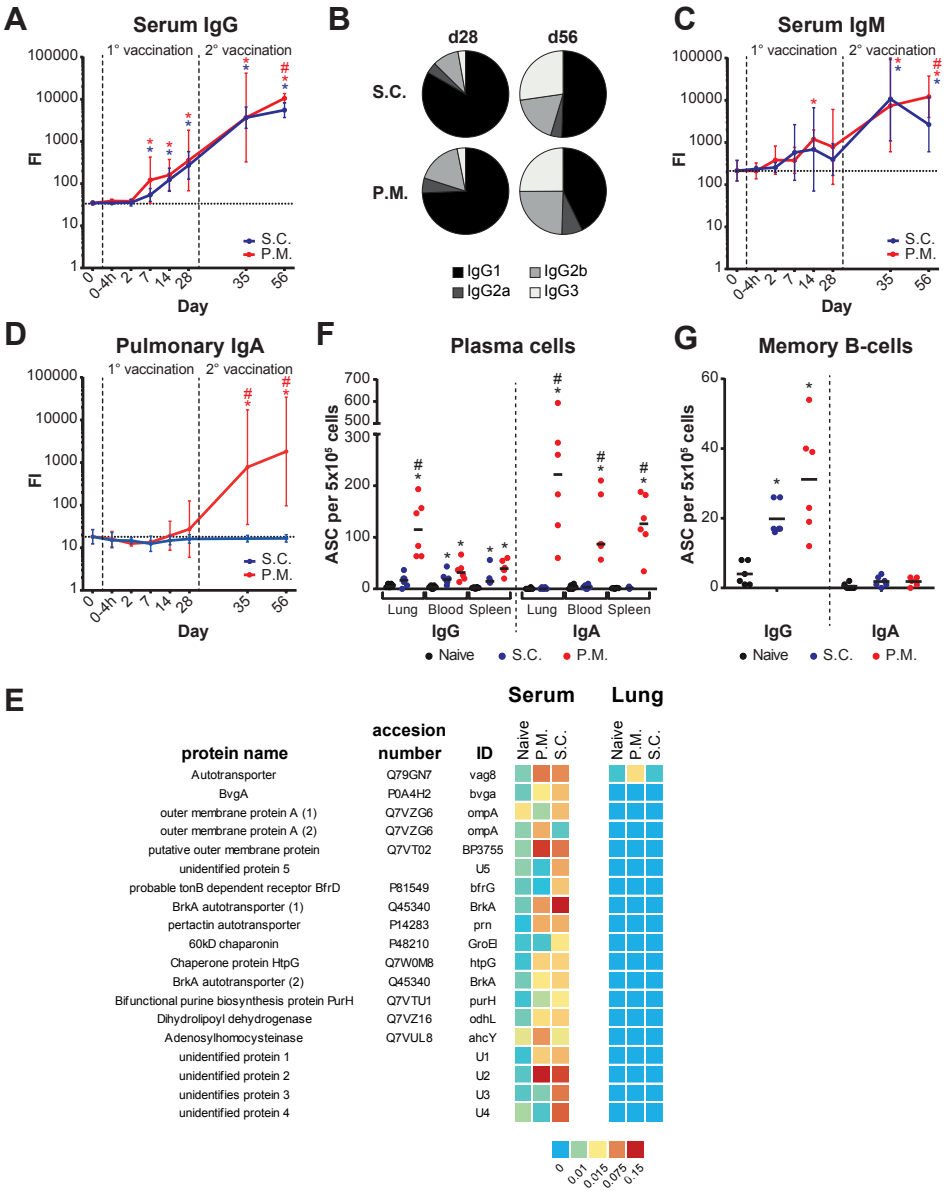

Figure 2 - *B. pertussis* OMV-specific B-cell responses induced by P.M. and S.C. immunization with omvPV. **(A-D)** By using MIA, **(A)** anti-OMV IgG antibody levels, **(B)** IgG subclass distribution, **(C)** IgM antibody levels were determined in sera and **(D)** anti-OMV IgA antibody levels in lung lysates. Results are expressed as fluorescence intensities (FI) of 4 mice per group per time point. **(E)** Specificity of serum IgG and pulmonary IgA elicited by P.M. and S.C. immunization as determined by 2DEWB. Analysis was performed using pooled serum and lung lysates of 4 mice per group. Fluorescence intensities for each spot were obtained from 1 blot for IgA and the average of 3 blots for IgG. * $p \leq 0.05$ versus naive mice (day 0); # $p \leq 0.05$ versus S.C. mice. **(F-G)** Numbers of **(F)** OMV-specific IgG- and IgA-secreting plasma cells in lungs, blood, and spleens and numbers of **(G)** IgG- and IgA-producing memory cells in spleens were determined by B-cell ELISpot of 6 mice per group at day 35 and day 56, respectively. Results are indicated as antibody secreting cells (ASC) per 5 x 10^5 cells. * $p \leq 0.05$ versus naive mice; # $p \leq 0.05$ versus S.C. mice.

Results

Superior protection against *B. pertussis* infection by P.M. compared to S.C. omvPV immunization

The colonization of the respiratory tract after intranasal *B. pertussis* challenge of pulmonary immunized mice (P.M. mice), subcutaneously immunized mice (S.C. mice), and non-immunized control mice (N.I. mice) differed substantially. Lungs, trachea, and noses of N.I. mice were heavily colonized by *B. pertussis* after a challenge. The highest numbers of colony forming units were found 7 days post challenge (p.c.) (**Figure 1B-D**). In contrast, *B. pertussis* was mostly cleared from lungs of P.M. mice already 2 days p.c., whereas bacteria from lungs of S.C. mice were cleared 5 days later (**Figure 1B**). In the trachea of both S.C. and P.M. mice, bacteria were mostly cleared 7 days p.c. (**Figure 1C**). In the nose, no complete clearance of *B. pertussis* was observed in the P.M., S.C., and N.I. mice within 28 days p.c. However, the number of bacteria in P.M. mice was significantly lower than in N.I. mice on day 70 (**Figure 1D**). Together, these data show that P.M. immunization with omvPV induced enhanced protection against *B. pertussis* infection compared to S.C. immunization.

IgG antibody responses

B. pertussis-specific antibodies are important contributors to pertussis immunity [34] and currently IgG serology still is the gold standard in pertussis vaccine research. The IgG (subclass) levels were determined after P.M. and S.C. immunization. Both immunization routes induced high and comparable levels of anti-OMV IgG antibodies in serum, but with significantly higher levels after P.M. immunization on day 56 (**Figure 2A**). S.C. immunization elicited already anti-Prn IgG antibodies after primary immunization, while these were observed only after a booster immunization in P.M. mice (**Figure S1A**).

The IgG subclasses distribution induced by P.M. and S.C. immunization were comparable for OMV-specific responses (**Figure 2B**). The primary immunization stimulated production of IgG1 antibodies, while the booster vaccination promoted the formation of IgG3 antibodies. For Prn-specific responses, booster P.M. immunization led to more IgG2a/b than S.C. immunization, while IgG1 still was the predominant subclass for both immunization routes (**Figure S1B**).

The immunogenic proteins to which the anti-OMV antibodies are directed were identified (**Figure 2E and Figure S3A-B**). On 2DEWB, twelve and seventeen immunogenic pertussis proteins were detected after P.M. and S.C. immunization, respectively (**Figure 2E and Table S1**). Spots showing high staining intensities in both groups corresponded with BP3755, Vag8, BrkA, and U2. Antibodies against ahcY, also visible at 55 kDa on 1DEWB (**Figure S3B**), and ompA(2) were solely induced by P.M. immunization, whereas antibody formation against ompA(1), U5, bfrG, GroEl, purH, U3, and U4 were only found after S.C. immunization. Additionally, anti-LPS antibodies (10 kDa) were observed after booster vaccination in both immunization groups (**Figure S3B**). Notably, following omvPV immunization via either route,

no IgG antibodies could be detected that were directed against Ptx, FHA, and Fim2/3 (data not shown), the antigens present in acellular pertussis vaccines in addition to Prn. Altogether, the systemic anti-OMV IgG response and subclass distribution after both P.M. and S.C. immunization were comparable and could not explain the increased protection of P.M. mice following challenge.

IgM antibody responses

Next, IgM antibodies were determined in sera from P.M. and S.C mice. IgM antibodies were only found directed against OMV and were induced significant on day 14 in P.M. mice. For both immunization routes, booster vaccination resulted in enhanced IgM antibody levels (**Figure 2C**). Similar to the findings for IgG, the level of anti-OMV IgM was significantly increased in P.M. versus S.C. immunized mice on day 56 (**Figure 2C**).

IgA antibody responses

IgA antibodies were found exclusively in P.M. mice, both in serum (**Figure S2A-B**) and lungs (**Figure 2D and S1D**). Serum IgA antibodies were directed against OMV and Prn, but not against other antigens present in acellular vaccines (**Figure S2A-E**). The specificity of pulmonary IgA was determined by immunoblotting and subsequent mass spectrometric identification of immunogenic proteins. The anti-OMV antibodies in the lungs were directed against Vag8 and LPS (**Figure 2E, S3A, and S3C**).

Pulmonary and systemic B-cell responses

The effect of the immunization route on the numbers of *B. pertussis*-specific plasma cells was investigated in cell suspensions from lungs, peripheral blood, and spleen. At the peak of the plasma cell response on day 35, anti-OMV and anti-Prn IgG-secreting cells were detected in the lungs of P.M. mice only (**Figure 2F and S1D**). However, in blood and spleen of S.C. and P.M. mice similar and modest numbers of IgG-secreting cells were found (**Figure 2F and S1D**). In addition, anti-OMV and anti-Prn IgA-secreting cells were detected in the lungs, spleen and blood, exclusively after P.M. immunization (**Figure 2F and S1D**).

Anti-OMV IgG-producing memory B-cells were measured in the spleen of P.M. and S.C. mice on day 56, with a trend towards higher numbers after P.M. immunization (**Figure 2G**). In contrast, anti-OMV IgA-producing memory B-cells could not be detected at all (**Figure 2G**). The Prn-specific memory B-cell responses on day 56 showed a similar trend as was found for the OMV-specific responses (**Figure S1G**). Thus, these data show that both S.C. and P.M. immunization elicited IgG-producing plasma and memory B-cells, while P.M. immunization also evoked IgA-producing plasma cells.

Pulmonary T-cell responses

Pulmonary *B. pertussis*-specific T-cell responses were investigated by analyzing cytokine

levels in the culture supernatants of lung cells that were restimulated with OMVs in vitro. Moderate IL-5 and vigorous IL-17A responses were detected after P.M. immunization only (Figure 3A). To investigate whether these cytokines were produced by $CD4^+$ T-cells, single cell analysis by ICS was performed on these cultured cells. Only P.M. immunization induced OMV-specific IL-17A-producing $CD4^+CD44^+$ T-cells in the lungs (Figure 3B). No OMV-specific IFNγ-producing and IL-5-producing $CD4^+CD44^+$ T-cells could be detected by ICS in the lungs of any of the immunized mice (data not shown).

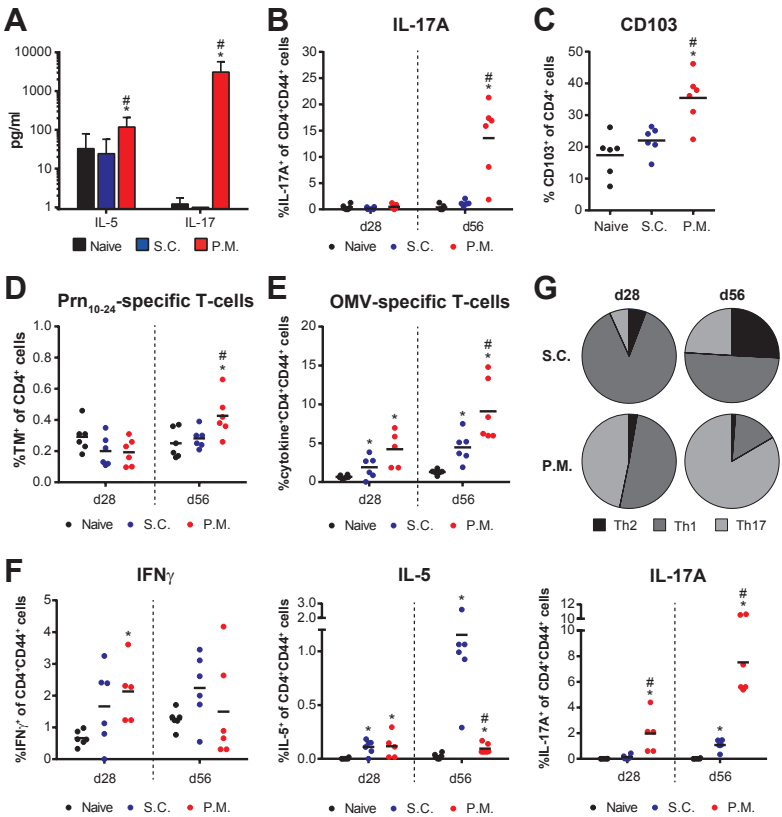

Figure 3 - Pulmonary and systemic *B. pertussis* OMV-specific T-cell responses induced by P.M. and S.C. omvPV immunization. **(A)** IL-5 and IL-17A levels in 3 day culture supernatant of lung cells, isolated on day 56, after *in vitro* stimulation with OMVs as determined by MIA. Results in pg/ml are corrected for the background level (IMDM complete medium control) and are given as mean ± SD of 6 mice per group. **(B)** Percentage of IL-17-producing $CD4^+CD44^+$ T-cells in the lungs, harvested on day 28 and day 56, as measured by ICS and flow cytometry after *in vitro* stimulation for 4 days with OMVs. **(C)** Flow cytometry for expression of CD103 on gated $CD4^+CD44^+$ T-cells in the lungs on day 56. **(D)** Frequency of Prn_{10-24}-specific $CD4^+$ T-cells in blood determined directly *ex vivo* on day 28 and day 56 using a tetramer staining and flow cytometry. **(E)** Magnitude of the systemic OMV-specific $CD4^+$ T-cell response after *in vitro* stimulation with OMV for 4 days was determined using ICS on splenocytes, calculated as the total percentage cytokine (IL-5, IFNγ, and IL-17A)-producing $CD4^+CD44^+$ T-cells. **(F)** Percentage IL-5-, IFNγ-, and IL-17-producing cells of $CD4^+CD44^+$ T-cells of spleens harvested on day 38 and day 56 and stimulated *in vitro* for 4 days with OMVs. Results of each analysis are given of 6 mice per group. **(G)** Distribution of Th subsets based on IL-5 (Th2), IFNγ (Th1), and IL-17A (Th17) production, as determined by ICS and flow cytometry. * $p \leq 0.05$ versus naive mice; # $p \leq 0.05$ versus S.C. mice.

Recently, it has been demonstrated that tissue-resident memory T-cells are important in the protection against respiratory pathogens [35]. Expression of CD103, a marker for tissue-resident memory T-cells, was determined on the OMV-specific IL-17A-producing $CD4^+CD44^+$ T-cells, which were solely detected in P.M. mice. Of these cells, 57 ± 24 percent expressed CD103 (data not shown). Moreover, an increased percentage of pulmonary $CD103^+CD4^+$ T-cells was detected in P.M. mice on day 56 compared to both S.C. and naive mice (**Figure 3C**). In conclusion, only P.M. immunization elicited pulmonary tissue-resident Th17 $CD4^+$ T-cells.

Magnitude of the systemic $CD4^+$ T-cell response

The magnitude of the Prn_{10-24}-specific $CD4^+$ T-cell response was determined *ex vivo* using tetramers specific for this immunodominant $I\text{-}A^d$ restricted T-cell epitope of Prn in BALB/c mice. No Prn_{10-24}-specific $CD4^+$ T-cells were detected in the dLN, bronchial and inguinal for P.M. and S.C. mice, respectively, on day 28 and day 56 (data not shown). However, Prn_{10-24}-specific $CD4^+$ T-cells were observed in blood of exclusively P.M. mice on day 56 (**Figure 3D**).

Furthermore, the magnitude of the $CD4^+$ T-cell response was investigated by determining the total percentage of *B. pertussis*-specific cytokine-producing (IFNγ, IL-5, or IL-17A) $CD4^+$ T-cells. Both P.M. and S.C. immunization induced a significant increase of OMV- and Prn-specific cytokine-producing $CD4^+CD44^+$ T-cells already on day 28 (**Figure 3E and S4B**). On day 56, a significantly higher percentage of these cells was detected after P.M. compared to S.C. immunization.

The effect of the immunization route on the Th-subset differentiation was determined. Analysis of cytokine levels in the culture supernatants of OMV-stimulated splenocytes revealed increased production of Th2 cytokine IL-4 and IL-5 after S.C. immunization, while the level of IL-13 was comparable after S.C. and P.M. immunization on day 28 and day 56 (**Figure S5A-B**). Stimulation of splenocytes with OMVs led to a high background production of Th1 cytokines IFNγ and TNFα of naive mice, possibly due to the presence of LPS in the OMVs (**Figure S5A-B**). Increased production of IFNγ by splenocytes from S.C. mice on day 28 and from P.M. on day 56 was still observed (**Figure S5A-B**). In addition, increased production of IL-17A and IL-10 was found by splenocytes of P.M. mice compared to S.C. mice on day 56. ICS analysis showed a significantly increased percentage of OMV-specific IFNγ-producing $CD4^+CD44^+$ T-cells after P.M. immunization on day 28 (**Figure 3F, left panel**). OMV-specific IL-5-producing $CD4^+CD44^+$ T-cells were detectable in P.M. and S.C. mice on day 28 and day 56. Notably, the percentage was significantly higher after S.C. immunization on day 56 (**Figure 3F, middle panel**). Significant OMV-specific IL-17A-producing $CD4^+CD44^+$ T-cells were induced after S.C. immunization on day 56. Notably, significantly higher percentages of these cells were detected after P.M. immunization at both day 28 and day 56 (**Figure 3F, right panel**). A similar trend for Prn-specific $CD4^+CD44^+$ T-cells were observed as the OMV-specific $CD4^+CD44^+$ T-cells (**Figure S4B**).

The distribution of OMV- and Prn-specific $CD4^+CD44^+$ T-cells, based on the production of

IFNγ, IL-5, or IL-17A, indicates that S.C. immunization induced systemically a Th1-dominated response on day 28 and a mixed Th1/Th17/Th2 response on day 56 (**Figure 3G and S4C**). In contrast, P.M. immunization induced a mixed Th1/Th17 response on day 28, which shifted towards a Th17-dominated response on day 56. In summary, more Th1/Th17-skewed $CD4^+$ T-cells were elicited by P.M. compared to S.C. immunization.

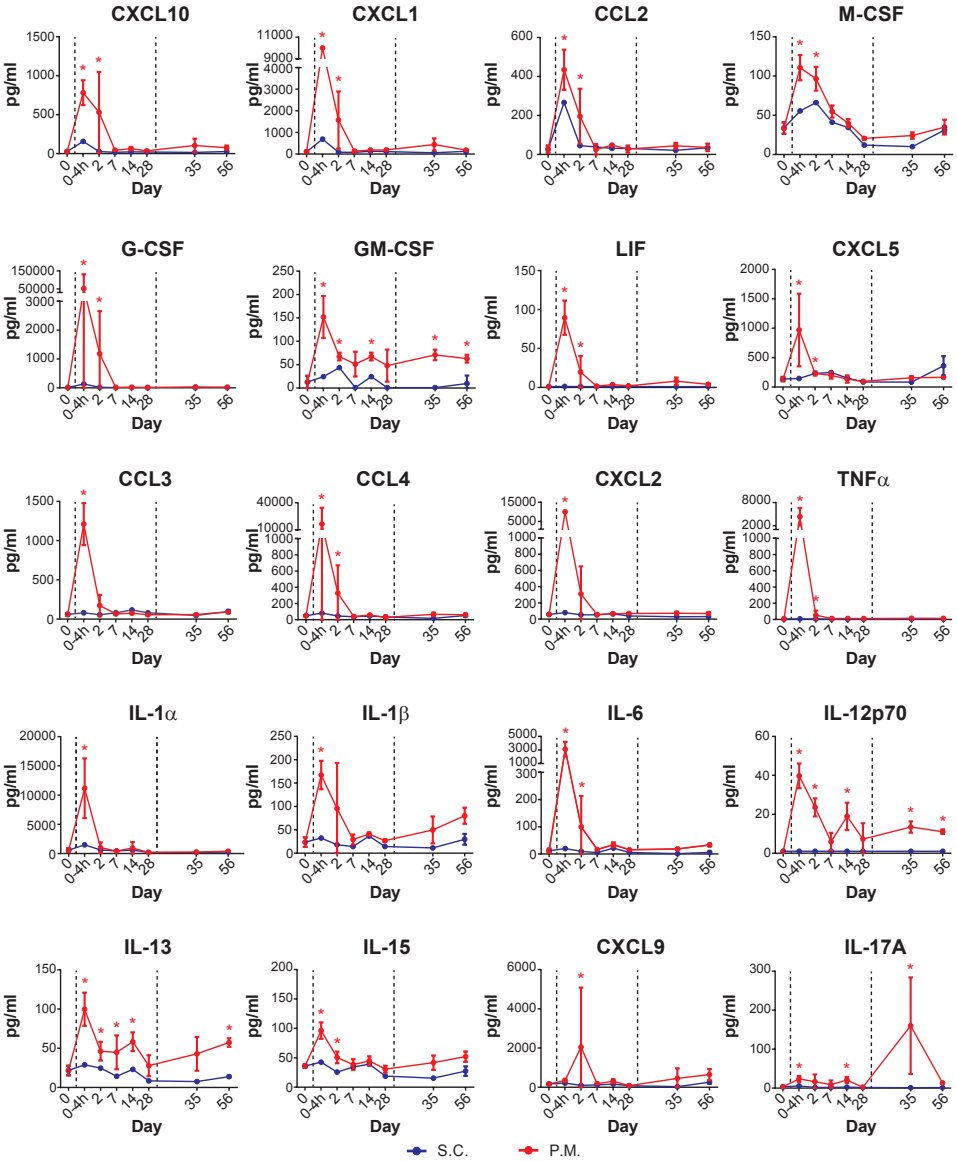

Figure 4 - Pulmonary cytokine responses after P.M. and S.C. omvPV immunization. The concentrations of cytokines in lung lysates of immunized mice were analyzed over time by using MIA. The cytokine concentrations were measured in the individual lung lysates of 4 mice per time point for P.M. mice and in a pool of the lung lysates of 4 mice per time point for S.C. mice.* $p \leq 0.05$ versus naive mice (day 0).

Cytokine profiles

The immunization-induced cytokine profile was determined in the lung lysates as well as serum. The largest differences were observed 4 hours post primary immunization (Figures 4 and 5). Concentrations of IL-6, IL-12p70, G-CSF, GM-CSF, IL-1α, IL-1β, IL-13, IL-15, LIF, CXCL5, CCL3, CCL4, CXCL2, CXCL10, CXCL1, CCL2, M-CSF, and TNFα were increased 4 hours post primary immunization in the lungs of P.M. mice. A trend towards increased levels of CXCL10, CXCL1, CCL2, and M-CSF was observed in the lungs of S.C. mice (Figure 4). At later time points, CXCL9 and IL-17A were found in P.M. mice on day 2 and day 35, respectively. In serum, increased levels of CXCL1, CCL4, TNFα, and IL-10 levels were found in both S.C. and P.M. mice (Figure 5A). In addition, higher levels of G-CSF, CXCL10, CCL2, CCL5, and IL-5 were detected after S.C. compared to P.M. immunization (Figure 5B), whereas the levels of IL-6 were higher in P.M mice (Figure 5C). Notably, CXCL1, CCL4, TNFα, G-CSF, CXCL10, CCL2, and IL-6 were found in both the lungs and sera of P.M. mice. Altogether, while S.C. induced only a systemic cytokine response, P.M. immunization induced a distinct systemic and pulmonary cytokine response.

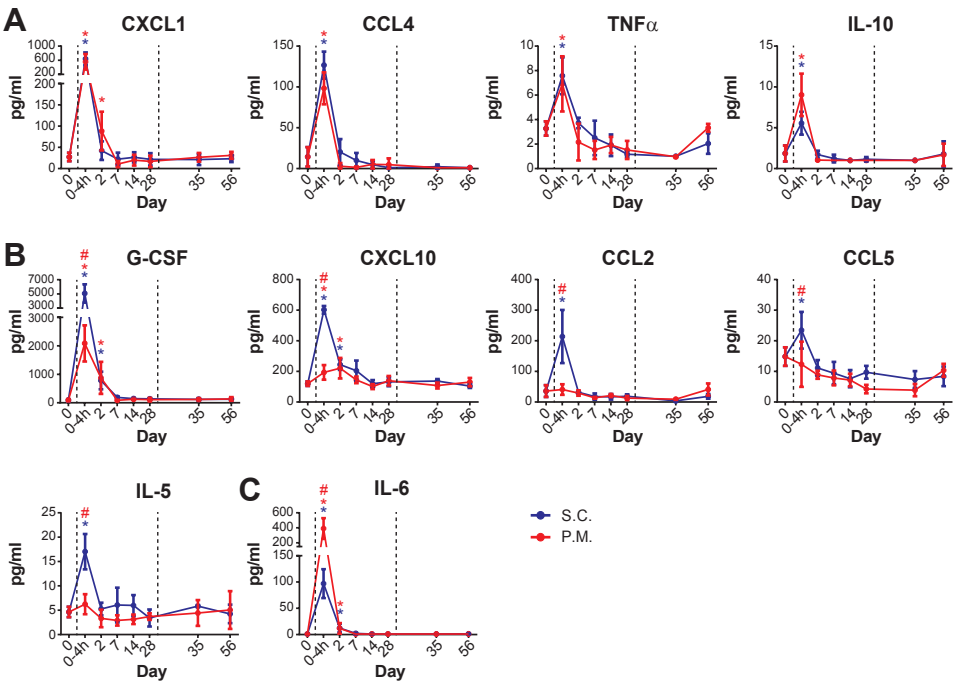

Figure 5 - Systemic cytokine responses after P.M. and S.C. omvPV immunization. The concentrations of cytokines in serum of immunized mice were analyzed over time by using MIA. **(A)** Cytokines with comparable levels in P.M. and S.C. mice. **(B)** Cytokines with elevated levels in S.C. compared to P.M. mice. **(C)** Cytokine with elevated level in P.M. compared to S.C. mice. Data is given as mean concentrations for 4 mice per group per time point. * $p \leq 0.05$ versus naive mice (day 0); # $p \leq 0.05$ versus S.C. mice.

Transcriptomic signatures in draining lymph nodes

Microarray analysis on bronchial and inguinal dLN from P.M. and S.C. mice, respectively, revealed 1921 genes that were differentially expressed (*p*-value ≤ 0.001, FR ≥ 1.5) over time compared to naive mice (**Figure 6A**). 951 genes were upregulated and 466 downregulated solely after P.M. immunization, 211 were upregulated and 145 were downregulated in both groups, and 109 were upregulated and 39 were downregulated exclusively after S.C. immunization. ORA using DAVID indicated enrichment of 141 GO-BP terms and KEGG pathways. A selection of these terms was sorted by the most significant enrichment and included Cell cycle, apoptosis, immune response, T-cell activation, and B-cell mediated immunity (**Figure 6B**). Cell cycle genes were mainly upregulated in P.M. mice. Innate signatures in the S.C. mice mainly involved genes downstream of IFN signaling (**Figure 6C**).

Genes related to T- and B-cells, based on gene ontology and text mining, are shown in **Figures 6D-E**. In total, 50 genes were related to T-cells of which many were associated with distinct Th subsets (**Figure 6D**). Upregulation of most genes occurred 4 hours after immunization and from day 7 onwards. More genes were upregulated in P.M. mice than in S.C. mice. The upregulated genes in P.M. mice included Th17-associated genes, such as the master regulator for Th17 differentiation (*Rorc*), *Hif1a*, and *Havcr1*. The few T-cell related genes exclusively expressed in S.C. mice comprised Th1- and Th17-associated genes, such as *Irf5, Ccr6,* and *Syt11*. Expression of B-cell related genes in S.C. mice mainly occurred on day 7 and day 35 (**Figure 6E**). In contrast, in P.M. mice elevated expression of B-cell related genes post primary immunization was detected earlier (4 hours) and persisted until day 28. Moreover, a smaller number of genes was induced on day 35 by booster immunization in P.M. compared to S.C. mice. Expression of *Mzb1, Ighm, Igkc, Ighg2b, Jchain, Ighg1,* and *Aicda* suggested antibody production and the presence of B-cells in dLN, which was more pronounced in P.M. mice. In addition, upregulation of specific B-cell membrane, activation, and homing markers were observed. Both immunization routes induced *Cxcr5, Cd22, Cd40,* and *Cd83* expression, while exclusively the S.C. route induced *Cd19, Cd72, Ccr6,* and *Siglecg* and exclusively the P.M. route induced *Cd38*.

In conclusion, P.M. and S.C. immunization with omvPV evoke distinct innate and adaptive responses in the dLN as detected on transcriptome level.

Figure 6 (Right) - Transcriptomic profiles in the draining lymph nodes following P.M. and S.C. omvPV immunization. **(A-E)** Gene expression in P.M. and S.C. mice was compared to naive mice (day 0) (FR ≥ 1.5, *p*-value ≤ 0.001). **(A)** 1921 genes upregulated (red) or downregulated (green) are visualized in heatmaps (mean of n = 3). Genes not surpassing a fold change of 1.5 are shown as basal level (black). The overlap (yellow) and the exclusive presence of genes in either the P.M. (blue) or S.C. (orange) immunization groups is depicted next to the heatmap. **(B)** Over-representation analysis on all 1921 genes revealed the involvement of specific GO-BP terms with corresponding total amount of genes (blue), upregulated (red) and downregulated (green) genes. **(C)** The 47 genes exclusively found upregulated during the innate response of the S.C. mice were shown in a heatmap (left panel) and the genes were compared to the Interferome database to determine involvement of the Type I IFN (IFNα and IFNβ) and/or Type II IFN (IFNγ) signaling pathway (right panel). **(D)** T-cell related genes, including association with distinct Th subsets, are depicted for P.M. and S.C. mice. **(E)** B-cell related genes are depicted for P.M. and S.C. mice.

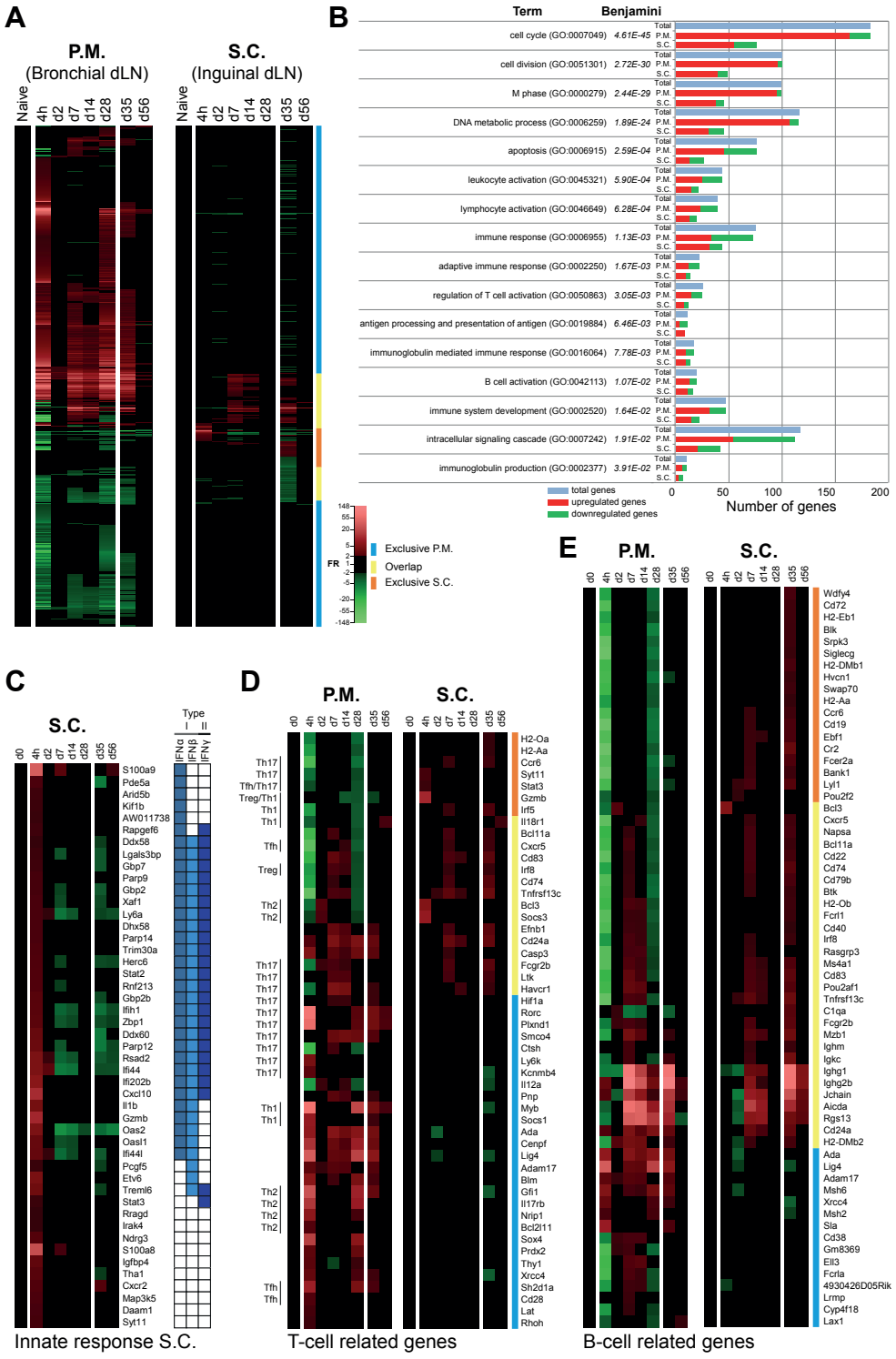
A
P.M.
(Bronchial dLN)
S.C.
(Inguinal dLN)
Naive
4h
d2
d7
d14
d28
d35
d56
B
Term
Benjamini
cell cycle (GO:0007049) 4.61E-45
cell division (GO:0051301) 2.72E-30
M phase (GO:0000279) 2.44E-29
DNA metabolic process (GO:0006259) 1.89E-24
apoptosis (GO:0006915) 2.59E-04
leukocyte activation (GO:0045321) 5.90E-04
lymphocyte activation (GO:0046649) 6.28E-04
immune response (GO:0006955) 1.13E-03
adaptive immune response (GO:0002250) 1.67E-03
regulation of T cell activation (GO:0050863) 3.05E-03
antigen processing and presentation of antigen (GO:0019884) 6.46E-03
immunoglobulin mediated immune response (GO:0016064) 7.78E-03
B cell activation (GO:0042113) 1.07E-02
immune system development (GO:0002520) 1.64E-02
intracellular signaling cascade (GO:0007242) 1.91E-02
immunoglobulin production (GO:0002377) 3.91E-02
Total
P.M.
S.C.
total genes
upregulated genes
downregulated genes
Number of genes
FR
Exclusive P.M.
Overlap
Exclusive S.C.
C
S.C.
Type
I
II
IFNα
IFNβ
IFNγ
Innate response S.C.
D
P.M.
S.C.
Th17
Tfh/Th17
Treg/Th1
Th1
Tfh
Treg
Th2
H2-Oa
H2-Aa
Ccr6
Syt11
Stat3
Gzmb
Irf5
Il18r1
Bcl11a
Cxcr5
Cd83
Irf8
Cd74
Tnfrsf13c
Bcl3
Socs3
Efnb1
Cd24a
Casp3
Fcgr2b
Ltk
Havcr1
Hif1a
Rorc
Plxnd1
Smco4
Ctsh
Ly6k
Kcnmb4
Il12a
Pnp
Myb
Socs1
Ada
Cenpf
Lig4
Adam17
Blm
Gfi1
Il17rb
Nrip1
Bcl2l11
Sox4
Prdx2
Thy1
Xrcc4
Sh2d1a
Cd28
Lat
Rhoh
T-cell related genes
E
P.M.
S.C.
Wdfy4
Cd72
H2-Eb1
Blk
Srpk3
Siglecg
H2-DMb1
Hvcn1
Swap70
H2-Aa
Ccr6
Cd19
Ebf1
Cr2
Fcer2a
Bank1
Lyl1
Pou2f2
Bcl3
Cxcr5
Napsa
Bcl11a
Cd22
Cd74
Cd79b
Btk
H2-Ob
Fcrl1
Cd40
Irf8
Rasgrp3
Ms4a1
Cd83
Pou2af1
Tnfrsf13c
C1qa
Fcgr2b
Mzb1
Ighm
Igkc
Ighg1
Ighg2b
Jchain
Aicda
Rgs13
Cd24a
H2-DMb2
Ada
Lig4
Adam17
Msh6
Xrcc4
Msh2
Sla
Cd38
Gm8369
Ell3
Fcrla
4930426D05Rik
Lrmp
Cyp4f18
Lax1
B-cell related genes

Pulmonary transcriptomic signatures

Microarray analysis was performed on lung tissue collected during the primary immunization and comprised 691 genes that were differentially expressed (*p*-value ≤ 0.01, FR ≥ 2.0) over time compared to naive mice (**Figure 7A**). The largest dissimilarity was observed 4 hours after P.M. immunization as revealed by a principal component analysis (PCA) (**Figure 7B**). Many of these genes were no longer expressed on day 2 and later, while upregulation of other genes was observed (**Figure 7A**), as was also observed in the direction of variance in the PCA (**Figure 7B**). The pulmonary gene expression on day 28 did not return completely to basal levels. Notably, also differential gene expression was observed mainly on day 2 in the lungs of S.C. mice (**Figure 7A-B**). ORA (Benjamini < 0.05) on the 691 genes revealed enrichment of 127 terms (11 KEGG Pathways, 116 GO-BP terms). A selection is shown in **Figure 7C**. Genes involved in pathogen recognition reflected by expression of PRR genes and members of corresponding downstream signaling pathways (inflammasome, TNF, NFκB, and MAPK) and effector molecules (e.g. pro-inflammatory responses) (**Figure 7C and S6A**). Moreover, genes involved in innate lymphoid cells (ILCs), CSF-signaling, T-cell activation, humoral response, and genes encoding complement, cytokines, cytokine receptors, and membrane markers were upregulated (**Figure 7C and S6B**).

The transcriptomic signatures obtained after P.M. immunization in the lungs (691 genes) were compared to the dataset of gene expression profiles (558 genes) discovered in the lungs of mice after experimental *B. pertussis* infection in a previous study [7]. In total, 98 genes were found in both datasets. A gene-function network analysis investigating the involvement of genes in modules PRR-signaling, acute phase, cytokine response, humoral response, and T-cell responses, showed differences between both datasets (**Figure 7D**). Notably, the infection dataset comprised more genes related to the modules acute phase and humoral response, whereas the P.M. immunization dataset included more genes related to cytokine response and PRR-signaling. Only a few shared genes (27 genes) were directly connected to the investigated modules. However, by using the STRING database many shared genes

Figure 7 (Right) - Pulmonary transcriptomic profiles following P.M. and S.C. omvPV immunization. **(A-C)** Gene expression was compared to naive mice (day 0) (FR ≥ 2.0, *p*-value ≤ 0.01). **(A)** 691 genes upregulated (red) or downregulated (green) are visualized in heatmaps (mean of n = 3 for P.M. mice and n = 1 (pool of 3 mice) for S.C. mice). Genes not surpassing a fold change of 2.0 are shown as basal level (black). **(B)** Principal component analysis (PC1 and PC2) shows the (dis)similarity of the five time points for both P.M. and S.C. mice. **(C)** ORA on 691 genes uncovered the involvement of specific GO-BP terms and KEGG pathways with corresponding total amount of genes (blue), upregulated (red) and downregulated (green) genes. **(D-E)** Pulmonary transcriptomes were compared after P.M. immunization and a *B. pertussis* infection [7]. **(D)** A gene-function network analysis showing the connection of genes, expressed within 28 days after P.M. immunization or infection, to a specific module (blue line) based on involvement in acute phase, cytokine response, humoral response, pathogen recognition receptor (PRR) signaling, and T-cell responses. Genes that were expressed in both datasets (shared, triangle, purple), exclusively expressed in infected mice (circle, green), or exclusively expressed in P.M. mice (circle, red) are depicted. Additional, indirect linkage of shared genes with other genes in the network (grey line) by using the STRING database are shown. **(E)** For infected mice (9 time points) and P.M. mice (6 time points) an average fold ratio (FR) (expressed as LN-transformed numbers) was calculated to determine the expression intensity and kinetics for each module corresponding to those included in the network analysis.

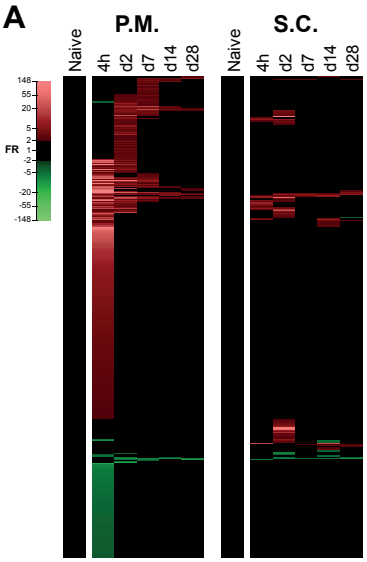
A
P.M.
S.C.
Naive
4h
d2
d7
d14
d28
FR
148
55
20
5
2
1
-2
-5
-20
-55
-148

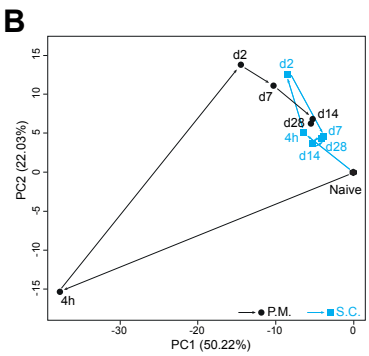
B
PC2 (22.03%)
PC1 (50.22%)
d2
d7
d14
d28
4h
Naive
P.M.
S.C.

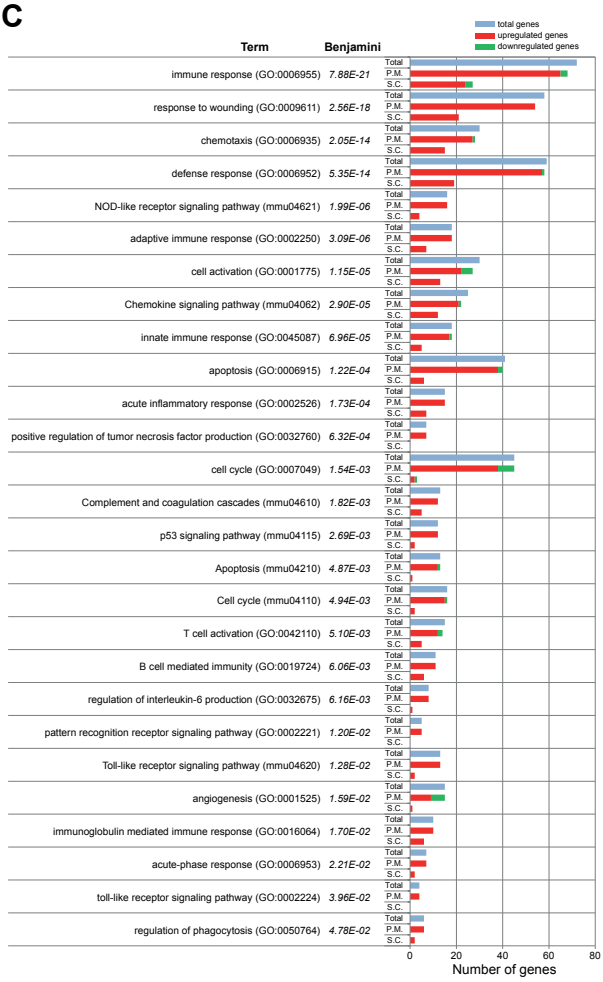
C
total genes
upregulated genes
downregulated genes
Term
Benjamini
immune response (GO:0006955) 7.88E-21
response to wounding (GO:0009611) 2.56E-18
chemotaxis (GO:0006935) 2.05E-14
defense response (GO:0006952) 5.35E-14
NOD-like receptor signaling pathway (mmu04621) 1.99E-06
adaptive immune response (GO:0002250) 3.09E-06
cell activation (GO:0001775) 1.15E-05
Chemokine signaling pathway (mmu04062) 2.90E-05
innate immune response (GO:0045087) 6.96E-05
apoptosis (GO:0006915) 1.22E-04
acute inflammatory response (GO:0002526) 1.73E-04
positive regulation of tumor necrosis factor production (GO:0032760) 6.32E-04
cell cycle (GO:0007049) 1.54E-03
Complement and coagulation cascades (mmu04610) 1.82E-03
p53 signaling pathway (mmu04115) 2.69E-03
Apoptosis (mmu04210) 4.87E-03
Cell cycle (mmu04110) 4.94E-03
T cell activation (GO:0042110) 5.10E-03
B cell mediated immunity (GO:0019724) 6.06E-03
regulation of interleukin-6 production (GO:0032675) 6.16E-03
pattern recognition receptor signaling pathway (GO:0002221) 1.20E-02
Toll-like receptor signaling pathway (mmu04620) 1.28E-02
angiogenesis (GO:0001525) 1.59E-02
immunoglobulin mediated immune response (GO:0016064) 1.70E-02
acute-phase response (GO:0006953) 2.21E-02
toll-like receptor signaling pathway (GO:0002224) 3.96E-02
regulation of phagocytosis (GO:0050764) 4.78E-02
Total
P.M.
S.C.
0
20
40
60
80
Number of genes

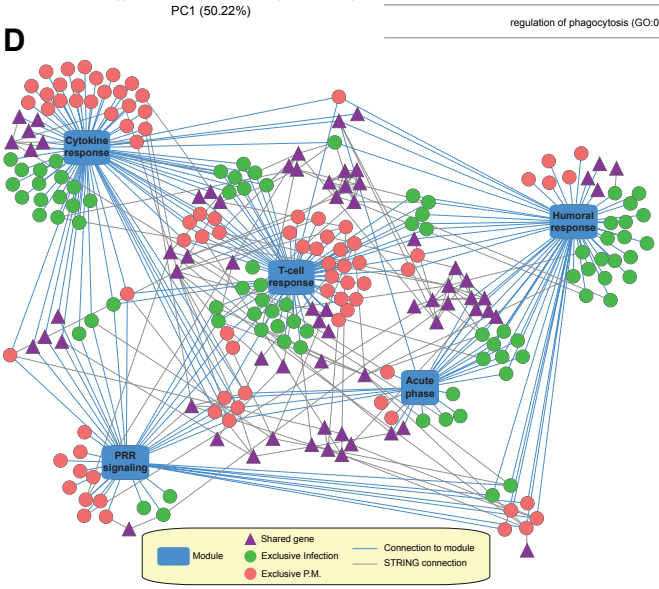
D
Cytokine response
T-cell response
Humoral response
Acute phase
PRR signaling
Module
Shared gene
Exclusive Infection
Exclusive P.M.
Connection to module
STRING connection

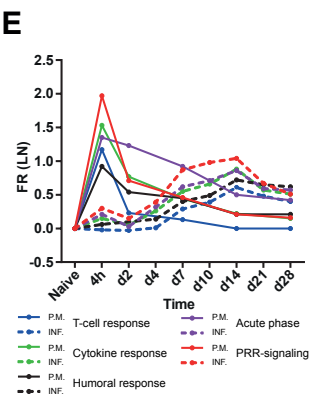
E
FR (LN)
2.5
2.0
1.5
1.0
0.5
0.0
-0.5
Naive
4h
d2
d4
d7
d10
d14
d21
d28
Time
P.M.
INF.
T-cell response
Acute phase
Cytokine response
PRR-signaling
Humoral response

(42 genes) could be indirectly linked to the modules by their interaction with other genes in the network. A comparison of intensity and kinetics of the average gene expression of each module revealed that P.M. immunization induced faster and more intense expression of all modules than infection (**Figure 7E**). In conclusion, both P.M. immunization and *B. pertussis* infection induced genes involved in PRR-signaling, acute phase, cytokine response, humoral response, and T-cell responses, yet with different intensity and kinetics. Moreover, the genes included in these modules are distinct for P.M. immunization and infection.

In vivo recall response after *B. pertussis* challenge

After unraveling the immune status of both of P.M. and S.C. mice on day 56, we determined the recall responses after an intranasal *B. pertussis* challenge. The serum anti-OMV IgG levels decreased after the challenge in P.M. and S.C. mice (**Figure 8A**). The challenge of non-immunized (N.I.) mice developed anti-OMV IgG and IgM, but the IgG levels remained lower compared to immunized mice (**Figure 8A**). For anti-Prn IgG levels a similar trend was observed after challenge (**Figure S1A**). However, no anti-Prn IgM was detected in any of the mice (data not shown). Further, no detectable levels of IgG and IgM to Ptx, FHA, or Fim2/3 were observed (data not shown). The challenge did not substantially alter the IgG subclass distribution of the anti-OMV and anti-Prn serum IgG response in P.M. and S.C. mice, present on day 56 (**Figure 2B and S1B**), since the IgG1 subclass remained dominant in both groups on day 84 (**Figure 8B and S1B**). However, a distinct distribution was found in challenged N.I. mice, since the IgG2b subclass response was more prominent in this group (**Figure 8B and S1B**). Enhanced serum IgA antibodies specific for OMV, Prn, and Fim2/3 were present in all challenged mice, whereas serum anti-Ptx and anti-FHA IgA were absent (**Figure S2A-E**). The pulmonary anti-OMV IgA antibody levels in P.M. mice remained high after the challenge, while in S.C. and N.I. mice these antibodies could only be detected on days 70 and day 84 (**Figure**

Figure 8 (Right) - *In vivo* recall response after *B. pertussis* challenge of P.M., S.C. and N.I. mice. **(A)** Serum anti-OMV IgG antibodies (left panel), IgM antibodies (middle panel), and pulmonary anti-OMV IgA antibodies (right panel) determined in time after *B. pertussis* challenge on day 56 using MIA. Results are expressed as fluorescence intensities (FI) of 4 mice per group per time point. * $p \leq 0.05$ versus levels on day 56; # $p \leq 0.05$ versus S.C. mice; + $p \leq 0.05$ versus N.I. mice. **(B)** Distribution of the anti-OMV IgG subclasses on day 84. **(C-D)** Numbers of OMV-specific IgG- and IgA-secreting plasma cells **(C)** and memory cells **(D)** in spleens on day 84, as determined by B-cell ELISpot of 6 mice per group. **(E)** Cytokine levels in 3 day culture supernatant of lung cells, isolated on day 84, after *in vitro* stimulation with OMVs, as determined by MIA. Results in pg/ml are corrected for the background level (IMDM complete medium control) and are given as mean ± SD of 6 mice per group. **(F)** Percentage of IL-17-producing $CD4^+CD44^+$ T-cells in the lungs, harvested on day 84, as measured by ICS and flow cytometry after *in vitro* stimulation for 4 days with OMVs. **(G)** Magnitude of the systemic OMV-specific $CD4^+$ T-cell response on day 84 after *in vitro* stimulation with OMV for 4 days, as determined by ICS on splenocytes and calculated as the total percentage cytokine (IL-5, IFNγ, and IL-17A)-producing $CD4^+CD44^+$ T-cells. **(H)** Distribution of Th subsets based on IL-5 (Th2), IFNγ (Th1), and IL-17A (Th17) production on day 84, as determined by using ICS and flow cytometry. * $p \leq 0.05$ versus naive mice; # $p \leq 0.05$ versus S.C. mice; + $p \leq 0.05$ versus N.I. mice. **(I)** The characteristics of the adaptive immune response obtained by primary (day 28) and booster (day 56) P.M. omvPV immunization in comparison to primary *B. pertussis* infection on day 28 and 56 are summarized. ‡ Obtained from a previous study [36]. N.D. = not determined.

8A). The same trend was observed for pulmonary anti-Prn IgA levels (Figure S1C). In addition, no pulmonary anti-Ptx and anti-FHA IgA antibodies were detected after challenge (data not shown), while pulmonary anti-Fim2/3 IgA antibodies were found in S.C. and N.I. mice on day 84 (Figure S2F). Anti-OMV IgA antibodies were only detected in nose lavages of P.M. mice 4 hours after challenge, which were most likely induced by the earlier immunization (Figure S7A). These nasal IgA antibodies were directed against Vag8 (Figure S3D) and Prn (Figure

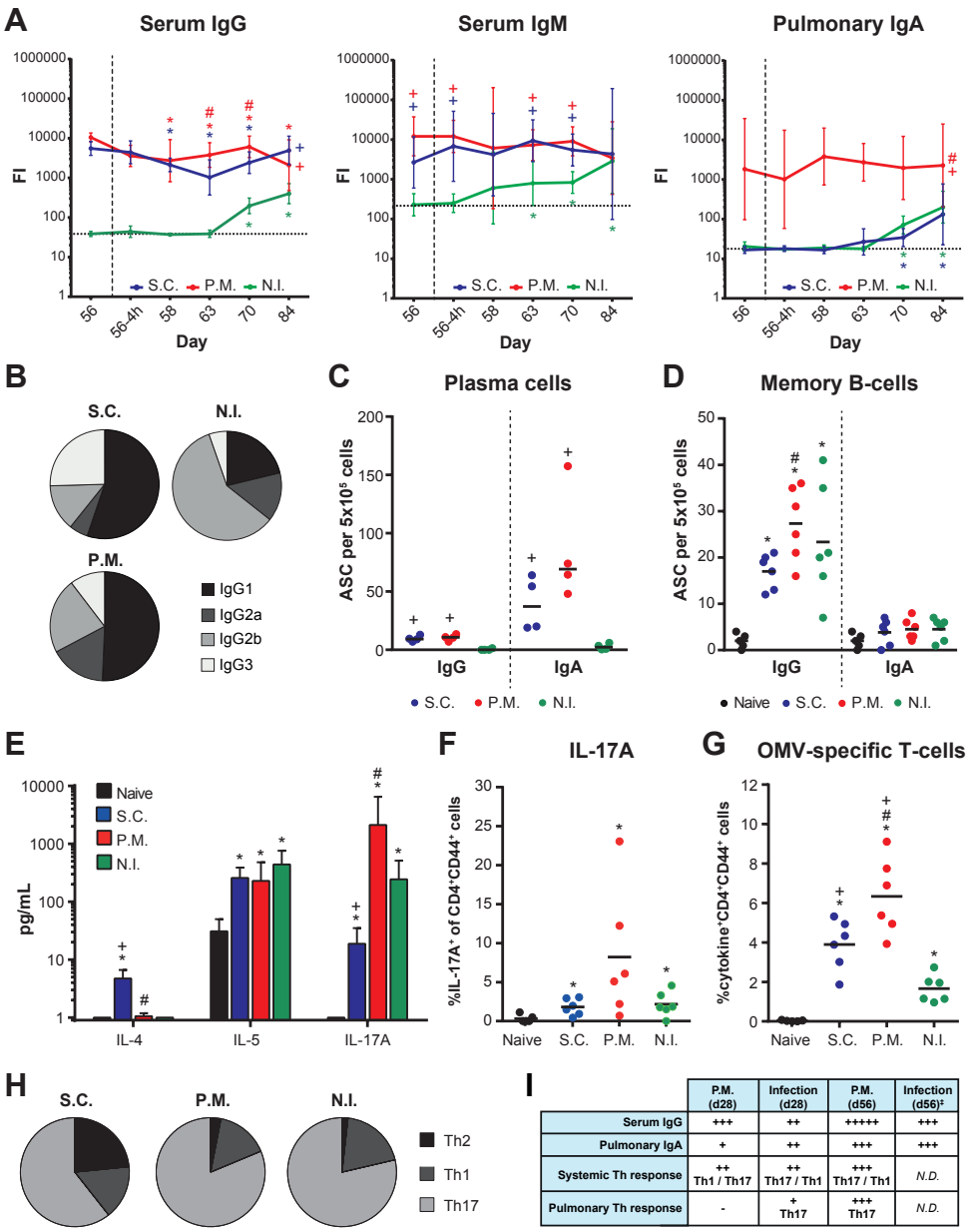

I

	P.M. (d28)	Infection (d28)	P.M. (d56)	Infection (d56)‡
Serum IgG	+++	++	+++++	+++
Pulmonary IgA	+	++	+++	+++
Systemic Th response	++ Th1 / Th17	++ Th17 / Th1	+++ Th17 / Th1	*N.D.*
Pulmonary Th response	-	+ Th17	+++ Th17	*N.D.*

S7B). The challenge led to enhanced anti-OMV IgA antibodies in all groups on day 84 (Figure S7A). In addition to higher anti-Vag8 IgA levels, the challenge induced anti-LPS antibodies in the P.M. and S.C. mice, but not in the N.I. control mice (Figure S3D). Furthermore, nasal anti-Prn, -Ptx, and -FHA IgA levels were significantly increased in S.C. mice following challenge (Figure S7B-D). Significantly higher anti-Fim2/3 IgA antibody concentrations were detected in N.I. mice on day 84 as compared to 4 hours after challenge, with the same trend in both immunized groups, but not significant (Figure S7E).

The numbers of anti-OMV IgG- and IgA-secreting plasma cells in the spleen of S.C. and P.M. mice were comparable and significantly higher than the numbers in N.I. mice on day 63 (Figure 8C). Furthermore, high numbers of anti-OMV IgG-producing memory B-cells were present in the spleen of P.M., S.C., and N.I. mice compared to the numbers in naive mice (Figure 8D). Moreover, higher numbers were induced by P.M. than S.C. immunization. In contrast, even after challenge, anti-OMV IgA-producing memory B-cells were not detected in any of the groups (Figure 8D). The Prn-specific antibody-secreting cells and memory B-cell responses showed a similar trend as found for the OMV-specific responses, except that no Prn-specific IgG-producing memory B-cells could be detected in challenged N.I. mice (Figure S1F-G).
Investigation of the culture supernatants of OMV-stimulated cells from the lungs showed IL-4 production solely by cells from S.C. mice (Figure 8E). In contrast, lung cells from all three challenged groups produced IL-5 and IL-17A, although IL-17A secretion by P.M. mice was significantly increased as compared to S.C. and N.I. mice (Figure 8E). However, a trend towards a higher percentage of OMV-specific IL-17A-producing $CD4^+CD44^+$ T-cells was observed in the lungs after challenge in P.M. compared to S.C. or N.I. mice (Figure 8F). Similar results were found after Prn stimulation, except that IL-17A-producing $CD4^+CD44^+$ T-cells were not detectable in N.I. mice (Figure S4C). OMV- and Prn-specific IFNγ- and IL-5-producing $CD4^+CD44^+$ T-cells were absent in the lungs of all challenged groups (data not shown). Systemic T-cell responses, as detected by ICS, showed a higher magnitude, as calculated by the total percentage of *B. pertussis*-specific cytokine-producing (IFNγ, IL-5, or IL-17A) splenic $CD4^+$ T-cells, in P.M. compared to S.C. and N.I. mice (Figure 8G). Moreover, distinct Th subset distributions were observed in S.C. and P.M. mice after challenge (Figure 8H). In S.C. mice, the pre-challenge Th response (Figure 3F) underwent a shift towards a Th17 response at the expense of the Th1 response. Notably, the Th2 component remained responsible for a quarter of the Th response. In P.M. mice, the Th response was not altered after challenge with little or no Th2 component (Figure 8H).

The systemic and local adaptive immune responses after a primary (day 28) and booster (day 56) P.M. immunization were schematically summarized and compared with those induced by a primary *B. pertussis* infection on day 28, obtained in this study, and day 56, obtained in our previous study [36]. The comparison demonstrated that the adaptive immune responses

were comparable after P.M. omvPV immunization and a *B. pertussis* infection (**Figure 8I**). Notably, there were however quantitative differences as the systemic IgG levels were higher after P.M. immunization compared to infection while pulmonary IgA levels were enhanced upon infection on day 28.

Collectively, the data of the *in vivo* recall responses indicate that the systemic and local memory B- and T-cell responses after P.M. versus S.C. omvPV-immunized mice were different in function and magnitude. The systemic ratio of the Th subsets and the IgA response induced by P.M. immunization was reminiscent of the response after primary *B. pertussis* infection.

Discussion

Pulmonary immunization induces local immunity important for protection as was demonstrated for several respiratory pathogens [11-13]. In this study, the immune responses evoked by pulmonary and subcutaneous immunization of an omvPV were compared in detail. Pulmonary immunization provided superior protection against *B. pertussis* challenge over the subcutaneous route. A systems biology approach revealed innate and adaptive immune signatures associated with this superior protection. The pulmonary gene expression and cytokine profiles exclusively evoked by P.M. immunization revealed omvPV recognition by PRRs, induction of pro-inflammatory and IL-17 effector cytokines, and IgA responses. Furthermore, in dLNs of S.C. mice, genes downstream of IFN signaling were expressed, while in dLNs of both P.M. and S.C. mice genes involved in the production of IgG were expressed. Moreover, based on gene expression, Th17-cells were detected in the dLNs of P.M. mice. The systemic cytokines, however, most were higher after S.C. immunization. Although both P.M. and S.C. immunization induced strong systemic adaptive immune response, P.M. immunization evoked higher IgM levels, IgG levels, and CD4+ T-cell responses. Moreover, the induced Th subsets differed, since P.M. immunization led to a mixed Th1/Th17, yet Th17 dominated, response, whereas S.C. immunization led to a mixed Th1/Th2/Th17 response. More importantly, P.M. immunization elicited a robust mucosal adaptive immune response as indicated by the presence of IgA antibodies, IgA- and IgG-producing plasma cells, and Th17 differentiated $CD4^+$ T-cells in the lungs of mice.

An overview of the main findings is presented in **Figure 9** and discussed in detail hereafter. During the innate phase, expression of genes associated with pathogen recognition and the PRR downstream-signaling cascade were detected in the lungs of P.M. mice, which included TLRs, MyD88, NFκB, and pro-inflammatory cytokines (**Figure 9A**). This demonstrates that the omvPV is sensed in the lung by TLR4, based on the expression of *Lbp* and *Cd14*, and by TLR2 on innate cells, which is similar to the recognition of wPV and whole bacteria [37-39]. Interestingly, also enhanced expression of *Tlr7* and *Nlrp3* was observed indicating activation of intracellular PRRs by omvPV. The expression of pro-inflammatory cytokines, such as *Il1b*, *Il6*, and *Cxcl10*, was also detected in the lungs on protein level. Multiple known IL-17 effector cytokines [8, 40] were measured in the lungs of P.M. mice, including CXCL1, CXCL2, CCL2, G-CSF, GM-CSF, and TNFα. These IL-17 effector cytokines facilitate, together with IL-1β and IL-6, a Th17-differentiating environment. This was reflected by the presence of Th17 cells in the dLN, based on expression of *Rorc*, *Hif1a*, and *Havcr1*. Moreover, Th17 cells were detected in the spleen and more importantly in the lungs on single cell level, suggesting induction of both systemic and tissue-resident cells. In addition, the presence of CCL3, CCL4, CXCL10, and IL-12p70 in the lungs promotes differentiation towards Th1 cells [41, 42]. Indeed Th1 differentiation was promoted, since Th1 cells were detected systemically on single cell level. A Th1/Th17 response is favorable for providing protection against *B. pertussis* infection [5, 7,

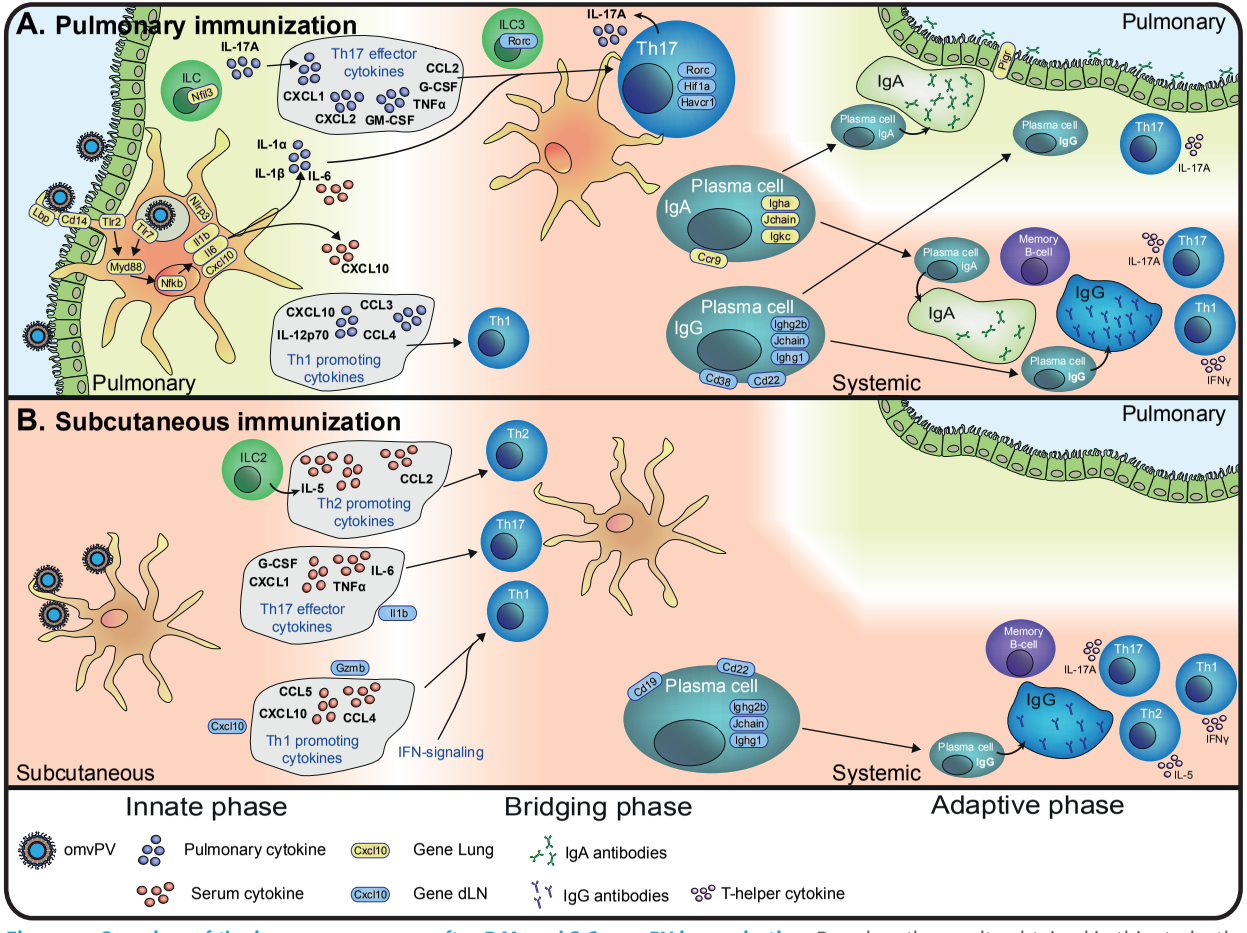

Figure 9 - Overview of the immune responses after P.M. and S.C. omvPV immunization. Based on the results obtained in this study, the main findings of the innate and adaptive immune responses were connected for **(A)** P.M. immunization and **(B)** S.C. immunization.

8] and additionally, the presence of tissue-resident T-cells in the lungs might even enhance protection [35]. The humoral response after P.M. immunization was characterized by pulmonary expression of IgA-related genes and the IgA transporter (*Pigr*) and the subsequent IgA presence in lungs and serum. In line with these findings, IgA-producing plasma cells were detected in spleen, blood, and lungs. Homing of these cells to the lungs may be enabled by CCR9, in our dataset found on gene expression level, which expression on IgA-producing memory B-cells is a mucosal homing marker. Furthermore, high serum IgG levels in P.M. mice corresponded with specific gene expression (*Ighg1, Igh2b,* and *Jchain*) of IgG-producing plasma cells in the dLN, and with detected IgG-producing plasma cells on single cell level in spleen, blood, and lungs. In addition, IgG-producing memory B-cells were detected in spleens of P.M. mice. Interestingly, pulmonary expression of *Nfil3* and early expression of *Rorc* in the dLN suggest involvement of ILCs in the immune response upon P.M. immunization. *Nfil3* is an ILC marker and *Rorc* is expressed by the ILC3 subset [43].

After S.C. immunization, omvPV is most likely sensed in a similar manner as after P.M. immunization, mainly by TLR2 and TLR4, although this was not investigated at the injection site in this study. The strong systemic cytokine response demonstrated a Th1- (CCL4, CCL5, and CXCL10), Th2- (IL-5 and CCL2), and Th17-differentiating (CXCL1, G-CSF, IL-6, and TNFα) environment, which was later reflected by presence of splenic Th1, Th2, and Th17 cells on single cell level (**Figure 9B**). Moreover, the induction of Th1 cells was linked to the early expression of genes downstream of IFN signaling found in the dLN [44]. The source of the early IL-5 production might be ILC2s [43], suggesting the involvement of these cells after S.C. omvPV immunization. Furthermore, the expression of B-cell markers (*Cd19* and *Cd22*) in addition to immunoglobulin-related genes (*Igh2b, Jchain,* and *Ighg1*) revealed the presence of IgG-producing plasma cells in the dLNs. Subsequently, IgG-producing plasma cells were detected on single cell level in spleen and blood. Additionally, S.C. omvPV immunization led to IgG-producing memory B-cells in the spleen and high serum IgG levels.

Based on the IgA responses, three interesting observations were revealed. First, full clearance of *B. pertussis* from the nose was not achieved despite the presence of anti-Vag8 IgA antibodies in the nose lavage in P.M. mice. This suggests that under the conditions used in our study with respect to vaccine and challenge dose, anti-Vag8 IgA induction in the nose alone may not be sufficient for prevention of nasal *B. pertussis* colonization. Second, 28 days after *B. pertussis* challenge, nasal anti-LPS IgA antibodies were detected in P.M. and S.C. mice, but not in non-immunized (N.I.) mice. Also, a lack of OMV-specific IgA-secreting plasma cells in N.I. mice after challenge was observed. Because no IgA response was detectable before challenge in S.C. mice, it was expected that challenge of S.C. and N.I. mice would evoke a similar IgA response. This faster induction of IgA responses in S.C. compared to N.I. mice may indicate the presence of low numbers of LPS-specific IgA-producing memory B-cells in S.C. mice stimulated upon a challenge. Third, large numbers of IgA-secreting plasma cells were present in the spleen 7 days post P.M. booster vaccination (day 35). However, IgA-producing

memory B-cells were non-detectable on day 56. Nonetheless, the recall of memory B-cells in response to infection led to a rapid increase in numbers of IgA-secreting plasma cells in the spleen (day 63). This suggests that IgA-producing memory B-cells may not reside in the spleen but elsewhere, presumably as tissue-resident IgA-producing memory B-cells in the mucosa [45]. Since IgA responses may contribute to protection against *B. pertussis* infection, these different aspects of the IgA responses require further investigation.

The immunity induced by P.M. immunization with an omvPV substantially resembles the infection-induced immunity, still considered as benchmark for optimal immunity. Interestingly, P.M. immunization with omvPV confers sterilizing immunity to a similar extent as is observed for infection-induced immunity in mice and baboons [5, 7, 8]. After both P.M. immunization and *B. pertussis* infection, a strong IgG response is induced. Furthermore, circulating and pulmonary IgA-producing B-cells were detected after P.M. immunization, leading to the production of mucosal IgA. This IgA was mainly directed against Vag8 as was observed after a challenge of mice with *B. pertussis* [36]. Moreover, both after P.M. immunization and *B. pertussis* infection, the $CD4^+$ T-cell responses, pulmonary and systemically, are Th17 dominated [5, 7, 8, 36].

Remarkably, there were also differences between P.M. immunization and infection-induced immunity. Serum IgG responses were already higher after primary P.M. immunization compared to *B. pertussis* infection on day 28. Moreover, increased IgG levels were found after booster immunization compared to the levels observed 56 days after infection [36]. Moreover, the omvPV vaccination in general evoked a distinct IgG subclass response compared to infection, which was partly caused by high anti-LPS IgG3 induction after the booster vaccination. IgG subclass distribution is thought to be indirect evidence for Th responses [46-48]. In our study the Th responses are not mirrored in the IgG subclass responses, since the Th responses are comparable after P.M. immunization and infection, while the IgG subclass distribution is distinct. Given that both S.C. and P.M. administration of omvPV result in an equal IgG subclass response, suggests that the differences compared to infection are probably caused by the vaccine composition and vaccination scheme rather than administration route. Furthermore, this study and our previous study [9] demonstrate that the antigen specificity of the serum IgG induced by P.M. immunization differs from infection, most likely due to distinct antigen composition. Whereas omvPV contains only outer-membrane and periplasmic proteins, live bacteria are comprised of additional cytosolic proteins and are capable of *de novo* production and secretion of antigens, such as Ptx [9]. Pulmonary IgA levels on day 28 induced by infection were higher compared to primary P.M. immunization. Booster P.M. immunization equalized the IgA levels with those after infection on day 56 [36].

Furthermore, with respect to cytokine profiles, P.M. immunization leads to faster and more intense pulmonary and serum cytokine production as compared to infection. However, higher

cytokine levels were expected during *B. pertussis* infection because of a prolonged antigen exposure [7] and a higher antigen dose compared to P.M. immunization with non-replicating omvPV. Weaker cytokine responses upon an infection might be explained by the immune evasion strategies of *B. pertussis* [49], such as dampening of host cytokine responses [50]. Extensive comparison of early pulmonary transcriptomic profiles induced by P.M. vaccination obtained from this study and those induced by *B. pertussis* infection [7] demonstrated that although both responses included genes involved in acute phase, PRR-signaling, cytokine responses, humoral response and T-cell responses, these responses comprised distinct genes. Moreover, P.M. immunization leads to faster and more intense pulmonary gene expression, which is in line with the cytokine profiles.
Together, the comparison of omvPV-induced immunity through P.M. administration and infection-induced immunity revealed overall comparability, notwithstanding some distinct innate responses.

Another advantage of pulmonary immunization, besides the induction of mucosal immune responses resembling that induced by *B. pertussis* infection, is that P.M. vaccine administration is needle-free. Currently, no pulmonary vaccines are licensed and only a few mucosal vaccines have been approved for human use. These include nasal vaccine against influenza virus and oral vaccines against poliovirus, rotavirus, *Salmonella typhi*, and *Vibrio cholerae* [51]. Pulmonary vaccine administration in humans is in early clinical development. Both powder inhalers [52] and fluid, nebulized vaccines are clinically tested, the latter in infants of 9 months of age [53]. Nasal vaccine administration might also be an option and may be suitable for infants. Intranasal immunization with an omvPV is also feasible since it provides protection against *B. pertussis* infection [14]. In addition, nasal immunization has been shown to result in IgA antibodies not only in the nasal cavity, but also lower in the respiratory tract [51, 54]. However, in depth analysis of the immune response induced by nasal immunization route in the context of pertussis is required.

In conclusion, this study showed that an omvPV can elicit superior local and systemic immunity against *B. pertussis* infection, with a similar type of adaptive immune response as induced by infection, by administering the vaccine pulmonary instead of subcutaneously. Therefore, pulmonary immunization may be key to the development of novel candidate pertussis vaccines. Further, in addition to serology, the gold standard in pertussis research, a systems biology approach is invaluable in order to unravel and understand the immunological signatures underlying the vaccine-induced immunity. In turn, this facilitates a rational choice for a vaccine candidate and route of administration, mitigating the risk of failure in the late-stage of development.

Acknowledgments

We are thankful to Tim Bindels and the employees of the Animal Research Centre (ARC) from Intravacc, Bilthoven, The Netherlands for respectively the production of the omvPV and performance of the animal experiments. We are grateful to Dale Long and Rick Willis of the NIH Tetramer Facility of Atlanta, Georgia, USA, for supplying the tetramers. We acknowledge the Microarray Department (MAD) of the University of Amsterdam, The Netherlands, for the performance of the microarray analyses.

References

1. Rumbo, M. and D. Hozbor, Development of improved pertussis vaccine. Hum Vaccin Immunother, 2014. 10(8): p. 2450-3.
2. Brummelman, J., *et al.*, Roads to the development of improved pertussis vaccines paved by immunology. Pathog Dis, 2015. 73(8): p. ftv067.
3. Mascart, F., *et al.*, Modulation of the infant immune responses by the first pertussis vaccine administrations. Vaccine, 2007. 25(2): p. 391-8.
4. Vermeulen, F., *et al.*, Cellular immune responses of preterm infants after vaccination with whole-cell or acellular pertussis vaccines. Clin Vaccine Immunol, 2010. 17(2): p. 258-62.
5. Ross, P.J., *et al.*, Relative contribution of Th1 and Th17 cells in adaptive immunity to *Bordetella pertussis*: towards the rational design of an improved acellular pertussis vaccine. PLoS Pathog, 2013. 9(4): p. e1003264.
6. Brummelman, J., *et al.*, Modulation of the CD4(+) T cell response after acellular pertussis vaccination in the presence of TLR4 ligation. Vaccine, 2015. 33(12): p. 1483-91.
7. Raeven, R.H.M., *et al.*, Molecular Signatures of the Evolving Immune Response in Mice following a *Bordetella pertussis* Infection. PLoS One, 2014. 9(8): p. e104548.
8. Warfel, J.M. and T.J. Merkel, *Bordetella pertussis* infection induces a mucosal IL-17 response and long-lived Th17 and Th1 immune memory cells in nonhuman primates. Mucosal Immunol, 2013. 6(4): p. 787-96.
9. Raeven, R.H.M., *et al.*, Immunoproteomic Profiling of *Bordetella pertussis* Outer Membrane Vesicle Vaccine Reveals Broad and Balanced Humoral Immunogenicity. J Proteome Res, 2015. 14(7): p. 2929-42.
10. Raeven, R.H.M., *et al.*, *Bordetella pertussis* outer membrane vesicle vaccine confers equal efficacy in mice with a lower inflammatory response compared to a classic whole-cell vaccine. Manuscript subitted.
11. Aguilo, N., *et al.*, Pulmonary but not subcutaneous vaccination confers protection to TB susceptible mice by an IL17-dependent mechanism. J Infect Dis, 2015.
12. Liu, H., *et al.*, Evaluation of mucosal and systemic immune responses elicited by GPI-0100- adjuvanted influenza vaccine delivered by different immunization strategies. PLoS One, 2013. 8(7): p. e69649.
13. Wang, J., *et al.*, Single mucosal, but not parenteral, immunization with recombinant adenoviral-based vaccine provides potent protection from pulmonary tuberculosis. J Immunol, 2004. 173(10): p. 6357-65.
14. Roberts, R., *et al.*, Outer membrane vesicles as acellular vaccine against pertussis. Vaccine, 2008. 26(36): p. 4639-46.
15. Asensio, C.J., *et al.*, Outer membrane vesicles obtained from *Bordetella pertussis* Tohama expressing the lipid A deacylase PagL as a novel acellular vaccine candidate. Vaccine, 2011. 29(8): p. 1649-56.
16. Asokanathan, C., M. Corbel, and D. Xing, A CpG-containing oligodeoxynucleotide adjuvant for acellular pertussis vaccine improves the protective response against *Bordetella pertussis*. Hum Vaccin Immunother, 2013. 9(2): p. 325-31.
17. Mielcarek, N., *et al.*, Live attenuated *B. pertussis* as a single-dose nasal vaccine against whooping cough. PLoS Pathog, 2006. 2(7): p. e65.
18. Querec, T.D., *et al.*, Systems biology approach predicts immunogenicity of the yellow fever vaccine in humans. Nat Immunol, 2009. 10(1): p. 116-25.
19. Furman, D., *et al.*, Apoptosis and other immune biomarkers predict influenza vaccine responsiveness. Mol Syst Biol, 2013. 9: p. 659.
20. Li, S., *et al.*, Molecular signatures of antibody responses derived from a systems biology study of five human vaccines. 2014. 15(2): p. 195-204.
21. Nakaya, H.I., *et al.*, Systems biology of vaccination for seasonal influenza in humans. Nat Immunol, 2011. 12(8): p. 786-95.
22. Lindqvist, M., *et al.*, Unraveling molecular signatures of immunostimulatory adjuvants in the female genital tract through systems biology. PLoS One, 2011. 6(6): p. e20448.
23. Brandes, M., *et al.*, A systems analysis identifies a feedforward inflammatory circuit leading to lethal influenza infection. Cell, 2013. 154(1): p. 197-212.
24. Sloots, A., *et al.*, Abolished pertactin cleavage enhances the immunogenicity and potency of a novel *B. pertussis* outer membrane vesicle vaccine: A proof of principle. Manuscript in preparation.
25. Thalen, M., *et al.*, Rational medium design for *Bordetella pertussis*: basic metabolism. J Biotechnol, 1999. 75(2-3): p. 147-59.
26. Bivas-Benita, M., *et al.*, Non-invasive pulmonary aerosol delivery in mice by the endotracheal route. Eur J Pharm Biopharm, 2005. 61(3): p. 214-8.
27. Stenger, R.M., *et al.*, Fast, antigen-saving multiplex immunoassay to determine levels and avidity of mouse serum antibodies to pertussis, diphtheria, and tetanus antigens. Clin Vaccine Immunol, 2011. 18(4): p. 595-603.
28. Stenger, R.M., *et al.*, Immunodominance in mouse and human CD4+ T-cell responses specific for the *Bordetella pertussis* virulence factor P.69 pertactin. Infect Immun, 2009. 77(2): p. 896-903.
29. Eijssen, L.M., *et al.*, User-friendly solutions for microarray quality control and pre-processing on ArrayAnalysis.org. Nucleic Acids Res, 2013. 41(Web Server issue): p. W71-6.
30. Bolstad, B.M., *et al.*, A comparison of normalization methods for high density oligonucleotide array data based on variance and bias. Bioinformatics, 2003. 19(2): p. 185-93.
31. Dai, M., *et al.*, Evolving gene/transcript definitions significantly alter the interpretation of GeneChip data. Nucleic Acids Res, 2005. 33(20): p. e175.
32. Huang da, W., B.T. Sherman, and R.A. Lempicki, Systematic and integrative analysis of large gene lists using DAVID bioinformatics resources. Nat Protoc, 2009. 4(1): p. 44-57.
33. Samarajiwa, S.A., *et al.*, INTERFEROME: the database of interferon regulated genes. Nucleic Acids Res, 2009. 37(Database issue): p. D852-7.
34. Plotkin, S.A., Complex correlates of protection after vaccination. Clin Infect Dis, 2013. 56(10): p. 1458-65.

35. Turner, D.L. and D.L. Farber, Mucosal resident memory CD4 T cells in protection and immunopathology. Front Immunol, 2014. 5: p. 331.
36. Raeven, R.H.M., *et al.*, Immunological signatures after *Bordetella pertussis* infection demonstrate importance of pulmonary innate immune cells. Manuscript subitted.
37. Brummelman, J., *et al.*, *Bordetella pertussis* naturally occurring isolates with altered lipooligosaccharide structure fail to fully mature human dendritic cells. Infect Immun, 2015. 83(1): p. 227-38.
38. Banus, S., *et al.*, The role of Toll-like receptor-4 in pertussis vaccine-induced immunity. BMC Immunol, 2008. 9: p. 21.
39. Higgins, S.C., *et al.*, TLR4 mediates vaccine-induced protective cellular immunity to *Bordetella pertussis*: role of IL-17-producing T cells. J Immunol, 2006. 177(11): p. 7980-9.
40. Tsai, H.C., *et al.*, IL-17A and Th17 cells in lung inflammation: an update on the role of Th17 cell differentiation and IL-17R signaling in host defense against infection. Clin Dev Immunol, 2013. 2013: p. 267971.
41. Rot, A. and U.H. von Andrian, Chemokines in innate and adaptive host defense: basic chemokinese grammar for immune cells. Annu Rev Immunol, 2004. 22: p. 891-928.
42. Christie, D. and J. Zhu, Transcriptional regulatory networks for CD4 T cell differentiation. Curr Top Microbiol Immunol, 2014. 381: p. 125-72.
43. Zhong, C. and J. Zhu, Transcriptional Regulatory Network for the Development of Innate Lymphoid Cells. Mediators Inflamm, 2015. 2015: p. 264502.
44. Huber, J.P. and J.D. Farrar, Regulation of effector and memory T-cell functions by type I interferon. Immunology, 2011. 132(4): p. 466-74.
45. Lamm, M.E. and J.M. Phillips-Quagliata, Origin and homing of intestinal IgA antibody-secreting cells. J Exp Med, 2002. 195(2): p. F5-8.
46. Mitsdoerffer, M., *et al.*, Proinflammatory T helper type 17 cells are effective B-cell helpers. Proc Natl Acad Sci U S A, 2010. 107(32): p. 14292-7.
47. Stevens, T.L., *et al.*, Regulation of antibody isotype secretion by subsets of antigen-specific helper T cells. Nature, 1988. 334(6179): p. 255-8.
48. Germann, T., *et al.*, Interleukin-12 profoundly up-regulates the synthesis of antigen-specific complement-fixing IgG2a, IgG2b and IgG3 antibody subclasses in vivo. Eur J Immunol, 1995. 25(3): p. 823-9.
49. de Gouw, D., *et al.*, Pertussis: a matter of immune modulation. FEMS Microbiol Rev, 2011. 35(3): p. 441-74.
50. Andreasen, C. and N.H. Carbonetti, Pertussis toxin inhibits early chemokine production to delay neutrophil recruitment in response to *Bordetella pertussis* respiratory tract infection in mice. Infect Immun, 2008. 76(11): p. 5139-48.
51. Holmgren, J. and C. Czerkinsky, Mucosal immunity and vaccines. Nat Med, 2005. 11(4 Suppl): p. S45-53.
52. Cape, S., *et al.*, Safety and immunogenicity of dry powder measles vaccine administered by inhalation: a randomized controlled Phase I clinical trial. Vaccine, 2014. 32(50): p. 6791-7.
53. Wong-Chew, R.M., *et al.*, Immunogenicity of aerosol measles vaccine given as the primary measles immunization to nine-month-old Mexican children. Vaccine, 2006. 24(5): p. 683-90.
54. Bergquist, C., *et al.*, Local and systemic antibody responses to dextran-cholera toxin B subunit conjugates. Infect Immun, 1995. 63(5): p. 2021-5.

Supplementary information

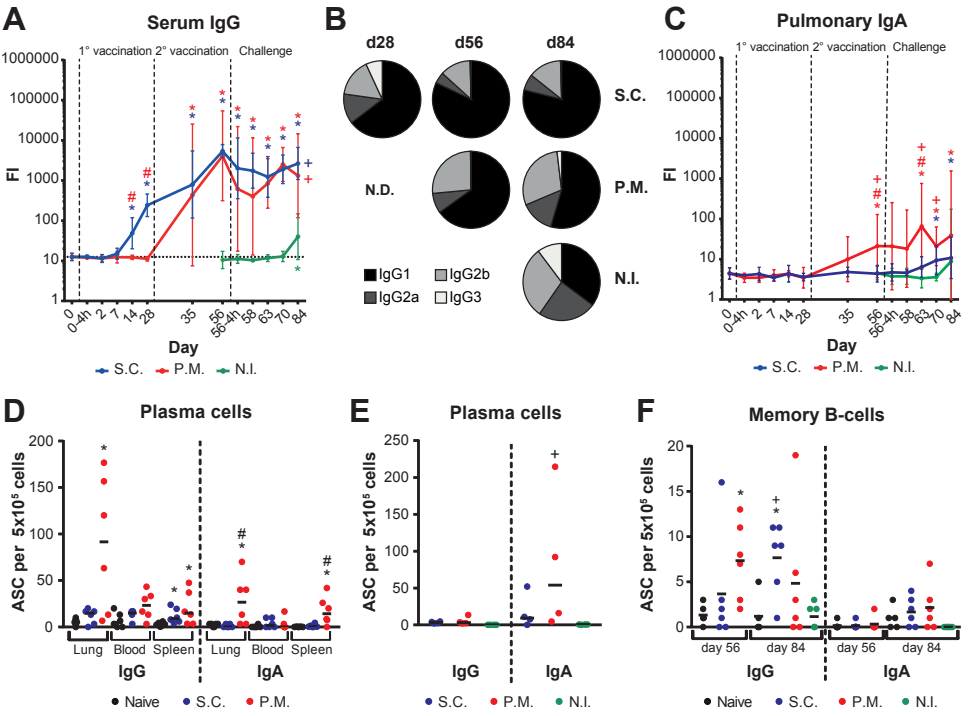

Figure S1 - Prn-specific B-cell responses induced by P.M. and S.C. omvPV immunization. **(A-C)** Serum anti-Prn IgG antibodies **(A)**, IgG subclass distribution **(B)**, and pulmonary anti-Prn IgA antibodies **(C)** were determined in immunized mice using MIA. Results are expressed as fluorescence intensities (FI) of 4 mice per group per time point. * $p \leq 0.05$ versus naive mice (day 0); # $p \leq 0.05$ versus S.C. mice; + $p \leq 0.05$ versus N.I. mice. **(D-E)** Numbers of Prn-specific IgG- and IgA-secreting plasma cells (n = 6) in **(D)** lungs, blood, and spleens on day 35 and in **(E)** spleens (n = 4) on day 63. **(F)** Numbers of Prn-specific IgG- and IgA-producing memory cells were determined in spleens (n = 6) on day 56 and 84. *$p \leq 0.05$ versus naive mice; # $p \leq 0.05$ versus S.C. mice; +$p \leq 0.05$ versus N.I. mice. N.D = not detected.

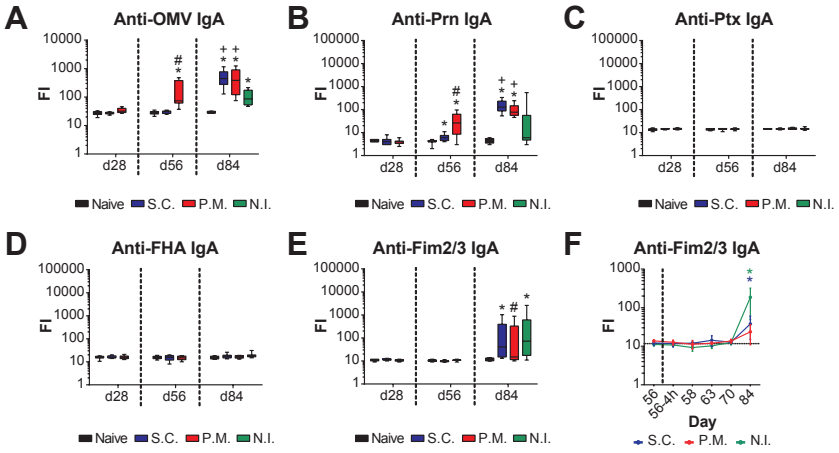

Figure S2 - Serum IgA levels against OMV, Prn, Ptx, FHA and Fim2/3 and pulmonary anti-Fim2/3 IgA induced by P.M. and S.C. omvPV immunization. **(A-E)** The levels of IgA antibodies directed against **(A)** OMV, **(B)** Prn, **(C)** Ptx, **(D)** FHA, and **(E)** Fim2/3 were determined in serum on day 28 and day 56 (vaccine-induced) and on day 84 (infection-induced) in naive, S.C., P.M., and N.I. mice. * $p \leq 0.05$ versus naive mice; # $p \leq 0.05$ versus S.C. mice; + $p \leq 0.05$ versus N.I. mice. **(F)** The levels of pulmonary anti-Fim2/3 IgA following challenge were determined in S.C., P.M. and N.I. mice. Results are expressed as fluorescence intensities (FI) of 4 mice per group per time point. * $p \leq 0.05$ versus levels day 56.

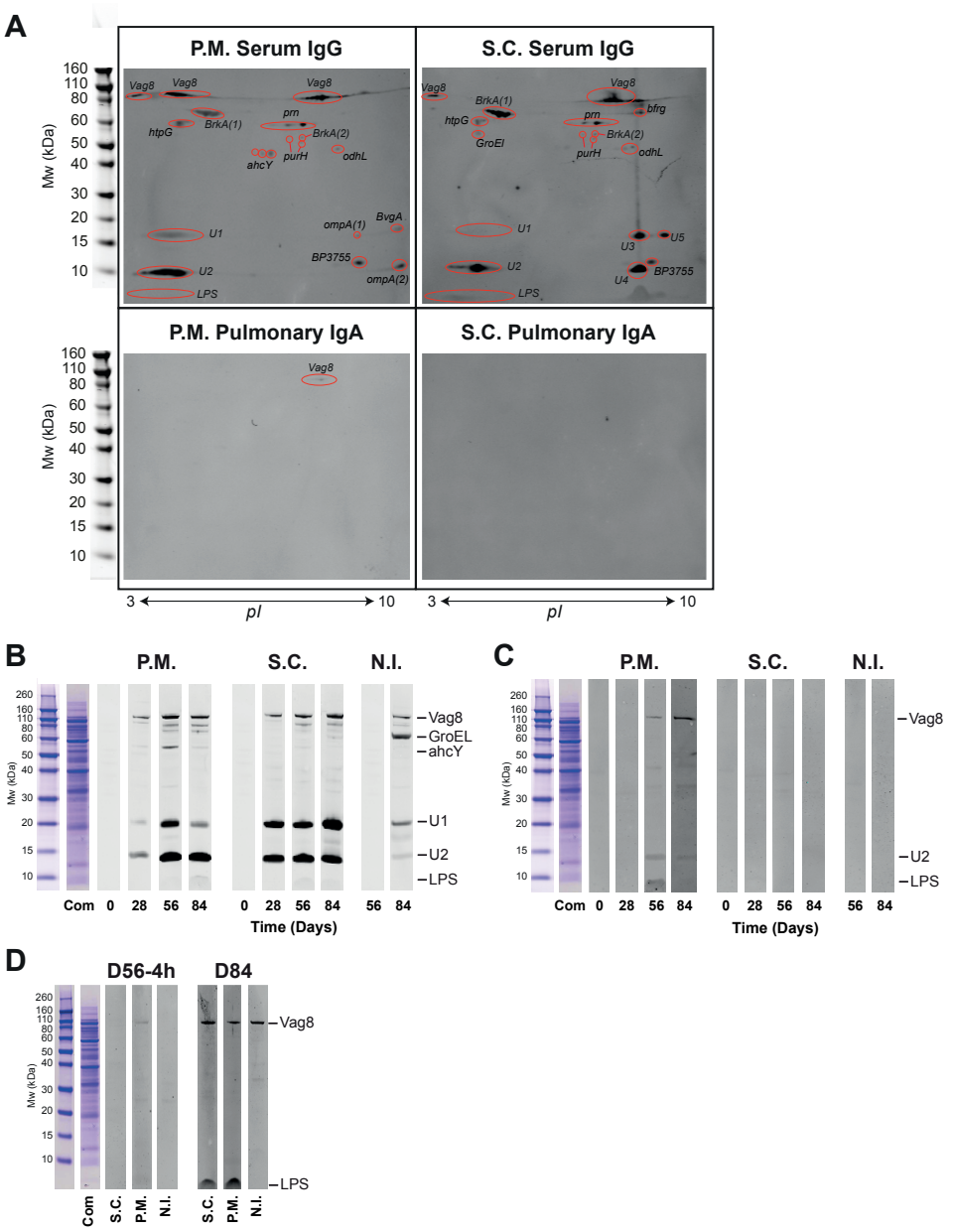

Figure S3 - Specificity of antibodies induced by P.M. and S.C. omvPV immunization. **(A)** Specificity of IgG and IgA in respectively serum and lung lysates of S.C. and P.M. mice on day 56 was determined using 2DEWB. Figure represents one blot for each condition. Individual spots with corresponding protein ID, as determined by LC-MS, are depicted. **(B-D)** Antibody specific as determined by 1DEWB for serum IgG **(B)** and pulmonary IgA **(C)** on day 28, 56, and 84 and nasal IgA **(D)** 4 hours and 28 days (day 84) after challenge. Identification of bands representing GroEL, LPS, Vag8, ahcY, and two unidentified antigens (U1-2) are shown. As a control a Coomassie staining (Com) was performed on the 1DE gel to stain the *B. pertussis* proteins.

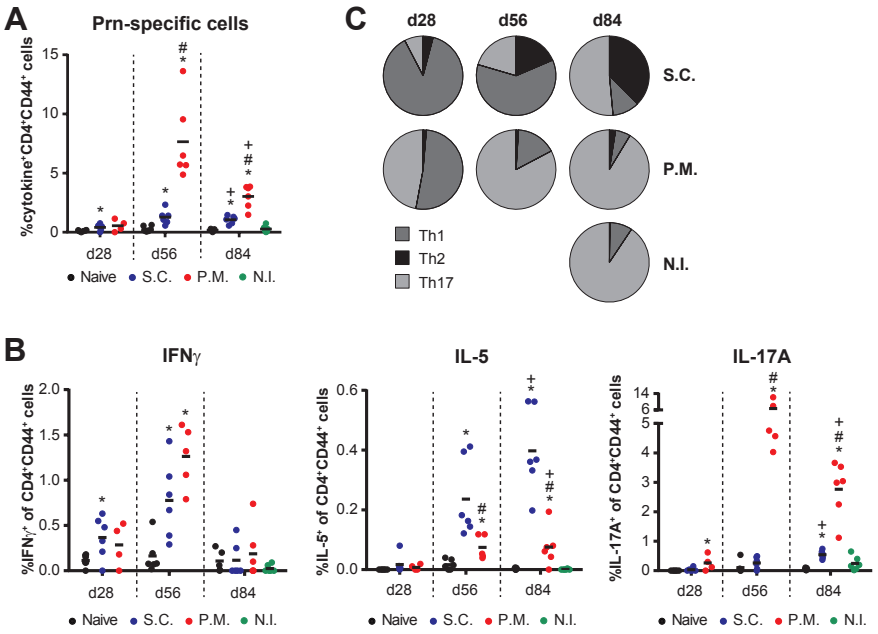

Figure S4 - Pulmonary and systemic Prn-specific T-cell responses induced by P.M. and S.C. omvPV immunization. **(A)** Magnitude of the Prn-specific $CD4^+$ T-cell response on day 28, 56, and 84 after *in vitro* stimulation with Prn for 4 days was determined using ICS and calculated as the total percentage cytokine (IL-5, IFNγ, and IL-17A)-producing $CD4^+CD44^+$ T-cells. **(B)** Percentage IL-5-, IFNγ-, and IL-17-producing cells of $CD4^+CD44^+$ T-cells of spleens harvested on day 38 and day 56 and stimulated *in vitro* for 4 days with Prn. Results of each analysis are given of 6 mice per group. **(C)** Distribution of Th subsets based on IL-5 (Th2), IFNγ (Th1), and IL-17A (Th17) production as determined using ICS and flow cytometry. * $p \leq 0.05$ versus naive mice; # $p \leq 0.05$ versus S.C. mice; + $p \leq 0.05$ versus S.C. mice.

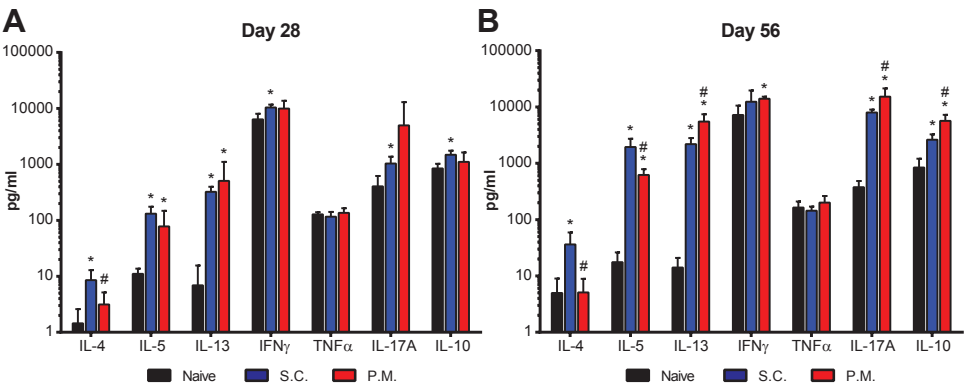

Figure S5 - Cytokine levels in supernatants of OMV stimulated splenocytes. **(A-B)** The presence of cytokines in day 3 culture supernatants of splenocytes collected on **(A)** day 28 and **(B)** day 56 was tested using a multiplex assay. Results in pg/ml are corrected for the background level (IMDM complete medium control) and are given as mean ± SD of 6 mice per group. * $p \leq 0.05$ versus naive mice; # $p \leq 0.05$ versus S.C. mice.

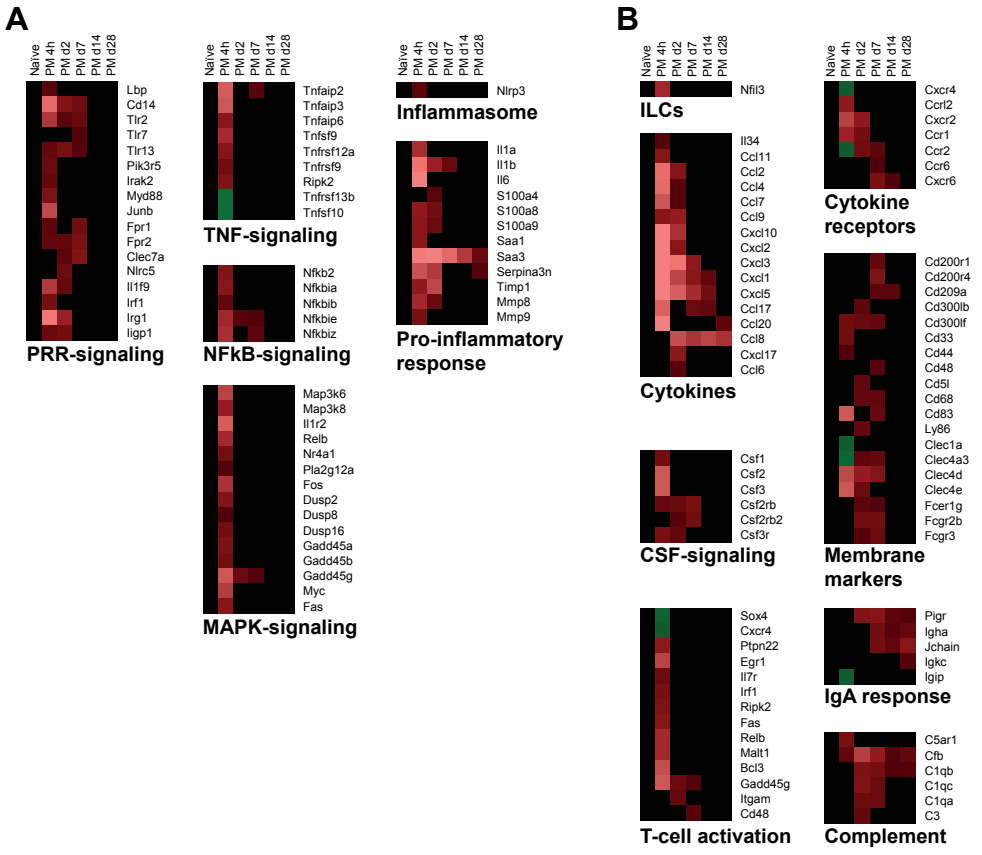

Figure S6 - Pulmonary transcriptome following P.M. immunization. **(A-B)** Differential upregulated (red) or downregulated (green) gene expression of P.M. mice (mean of n = 3) compared to naive mice (day 0) (FR ≥ 2.0, *p*-value ≤ 0.01). Genes not surpassing a fold change of 2.0 are shown as basal level (black). **(A)** Genes are depicted involved in pathogen recognition, such as the inflammasome and the pathogen recognition receptor (PRR)-, TNF-, NFκB-, and MAPK-signaling pathways and pro-inflammatory responses. **(B)** Genes are depicted involved in ILCs, CSF-signaling, T-cell activation, humoral response, and complement in addition to genes encoding for cytokines, cytokine receptors, and membrane markers.

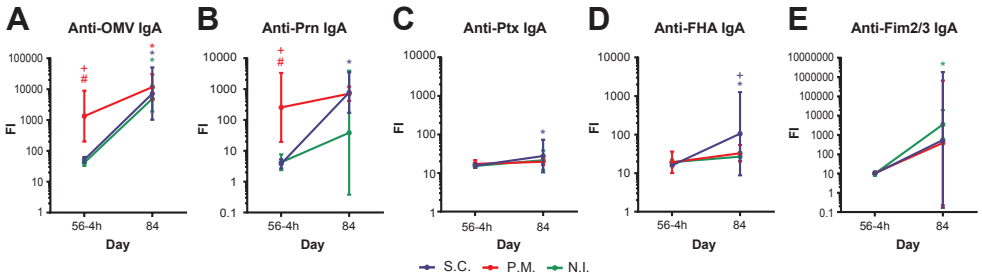

Figure S7 - IgA responses in the nose lavages of P.M., S.C., and N.I. mice. IgA antibodies specific for OMV **(A)**, Prn **(B)**, Ptx **(C)**, FHA **(D)**, and Fim2/3 **(E)** were determined in the nose lavage of P.M., S.C., and I.N. mice 4 hours after *B. pertussis* challenge (d56-4h) and at day 84. Results are expressed as fluorescence intensities (FI) of 4 mice per group per time point. * $p \leq 0.05$ versus levels on d56-4h; # $p \leq 0.05$ versus S.C. mice; + $p \leq 0.05$ versus N.I. mice.

Table S1 Immunogenic proteins determined by LC/MS of excised spots found by immunoblotting of 2DE gels

protein description[a]	accession number[b]	ID[b]	Mw (kDA)[c]	pI[c]	coverage (%)[d]	number of peptides assigned with high confidence[d]
60kD chaparonine	Q7W0M8	*GroEl*	57.4	5.2	69	33
adenosylhomocysteinase	Q7VUL8	*ahcY*	51.6	6.1	53	20
autotransporter	Q79GN7	*vag8*	94.8	6.8	41	27
bifunctional purine biosynthesis protein	Q7VTU1	*purH*	55.8	6.3	36	16
BrkA autotransporter (1)	Q45340	*BrkA*	103.3	7.1	30	21
BrkA autotransporter (2)	Q45340	*BrkA*	103.3	7.1	18	14
chaperonine protein HtpG	Q7W0M8	*htpG*	71.1	5.2	65	39
dihidrolipoyl dehydrogenase	Q7VZ16	*odhL*	50.1	6.8	61	25
outer membrane protein A (1)	Q7VZG6	*ompA*	21.0	8.7	17	3
outer membrane protein A (2)	Q7VZG6	*ompA*	21.0	8.7	35	5
pertactin autotransporter	P14283	*prn*	93.4	9.2	28	16
probable tonB dependent receptor	P81549	*BfrD*	79.3	8.2	58	37
putative outer membrane protein	Q7VT02	*BP3755*	23.0	9.2	26	5
Virulence factors putative positive transcription regulator	P0A4H2	*bvga*	22.9	8.4	78	14

a) Proteins in excised gel spots identified by LC–MS analysis.
b) Accession numbers of proteins and corresponding ID provided by uniprot (http://www.uniprot.org).
c) Molecular weight (Mw) and isoelectric point (pI) are calculated based on protein sequence.
d) Percentage of a protein sequence covered by identified peptides from the corresponding protein and the number of peptides assigned with high confidence.

About the cover: The Jet d' Eau fountain in Geneva, Switserland. The 140 metres high fountain is located in the Lake Geneva. In 2015, René was invited to participate in the roundtable discussion at the Foundation Merieux event "*Pertussis: biology, epidemiology and prevention*" that was held in Annecy, France.